The cellular Notch1 Protein Promotes KSHV reactivation in an Rta-dependent manner.

Jennifer DeCotiis-Mauro[a,b], Sun M. Han[a,b]+, Helena Mello[a,b]+, Corey Goyeneche[a,b], Giuseppina Marchesini-Tovar[a,b], Lianhua Jin[a,b], Vivian Bellofatto[a,b], and David M. Lukac[a,b]#

[a] Dept of Microbiology, Biochemistry, and Molecular Genetics, Rutgers Biomedical and Health Sciences, New Jersey Medical School, Rutgers University, Newark, NJ

[b]School of Graduate Studies, Rutgers Biomedical and Health Sciences, Health Science Campus at Newark, Rutgers University, Newark, NJ

Running Head: Notch1 contributes to KSHV reactivation

#Corresponding author: E-mail: Lukacdm@njms.rutgers.edu

+ authors contributed equally to this work

Abstract: 245 words

Abstract

The cellular Notch signal transduction pathway is intimately associated with infections by Kaposi's sarcoma-associated herpesvirus (KSHV) and other gamma-herpesviruses. RBP-Jk, the cellular DNA binding component of the canonical Notch pathway, is the key Notch downstream effector protein in virus-infected and uninfected animal cells. Reactivation of KSHV from latency requires the viral lytic switch protein, Rta, to form complexes with RBP-Jk on numerous sites within the viral DNA. Constitutive Notch activity is essential for KSHV pathophysiology in models of Kaposi's sarcoma (KS) and Primary Effusion Lymphoma (PEL), and we demonstrate that Notch1 is also constitutively active in infected Vero cells. Although the KSHV genome contains >100 RBP-Jk DNA motifs, we show that none of the four isoforms of activated Notch can productively reactivate the virus from latency in a highly quantitative trans-complementing reporter virus system. Nevertheless, Notch contributed positively to reactivation because broad inhibition of Notch1-4 with gamma secretase inhibitor (GSI) or expression of dominant negative mastermind-like1 (dnMAML1) coactivators severely reduced production of infectious KSHV from Vero cells. In infected PEL cells, we show that reduction of vDNA synthesis by GSI is associated with gene specific reduction of viral transcription. Specific inhibition of Notch1 by siRNA partially reduces production of infectious KSHV, and ectopic activated Notch (NICD1) enhances virus production induced by Valproic Acid (VPA) treatment. We conclude that constitutive Notch activity is required for robust production of infectious KSHV, and our results implicate activated Notch1 as a pro-viral member of a MAML1/RBP-Jk complex during viral reactivation.

51 **Importance**

52 Kaposi's sarcoma-associated herpesvirus (KSHV) manipulates the host cell oncogenic Notch
53 signaling pathway for viral reactivation from latency and cell pathogenesis. KSHV reactivation requires
54 that the viral protein Rta functionally interacts with RBP-Jk, the DNA binding component of the Notch
55 pathway, and with promoter DNA to drive transcription of productive cycle genes. We show that the
56 Notch pathway is constitutively active during KSHV reactivation and is essential for robust production
57 of infectious virus progeny. Inhibiting Notch during reactivation reduces expression of specific viral
58 genes yet does not affect growth of the host cells. Although Notch cannot reactivate KSHV alone, the
59 requisite expression of Rta reveals a previously unappreciated role for Notch in reactivation. We
60 propose that activated Notch cooperates with Rta in a promoter-specific manner that is partially
61 programmed by Rta's ability to redistribute RBP-Jk DNA binding to the virus during reactivation.
62

63 **Introduction**

64 Human gammaherpesviral infections and pathogenesis are dependent on interactions of the virus
65 with the cellular Notch signal transduction pathway (1). In uninfected cells, the canonical model of
66 Notch signaling involves activation of the Notch protein by proteolytic release of the Notch Intracellular
67 Domain (NICD)1 from the membrane-associated Notch1 receptor (2, 3). NICD1 then translocates to the
68 cell nucleus, binds to DNA-bound Recombination signal binding protein (RBP)-Jk and activates
69 transcription by displacing a transcriptional co-repressor complex from RBP-Jk and assembling a
70 transcriptional co-activator complex.

71 Reactivation of the gammaherpesvirus Kaposi's sarcoma-associated herpesvirus (KSHV)
72 requires the KSHV Replication and transcriptional activator (Rta) to assemble a complex with RBP-Jk
73 and DNA to activate transcription of essential viral genes (4-25). Reflecting the central roles of Rta and
74 RBP-Jk in reactivation, the KSHV genome contains greater than 100 consensus RBP-Jk DNA motifs,
75 and Rta and RBP-Jk co-occupy many viral promoters during reactivation in B cells (26). However,
76 although both Rta and NICD1 target RBP-Jk, we and others have shown that only Rta is sufficient to
77 productively reactivate KSHV in B cell models of latency (4, 27). Indeed, our recent work showed that
78 ectopic expression of Rta in infected Vero cells induced profound production of infectious virus assayed
79 by a robust and sensitive trans-complementing reporter virus-cell system (28). In parallel experiments,
80 this highly sensitive assay revealed that ectopic expression of NICD1 failed to produce detectable virus
81 (28). Thus, this highly sensitive reactivation system confirmed conclusions from human B cell studies
82 and is ideal to compare transcriptional mechanisms of Rta and Notch.

83 Despite ectopic NICD1's insufficiency to reactivate KSHV alone, the literature suggests that
84 Notch signaling contributes to regulation of KSHV infection. Notch can activate viral productive cycle
85 genes without inducing complete reactivation in B and endothelial cell models of latency (27, 29). In
86 infected primary effusion lymphoma (PEL) cells, conditionally-expressed NICD1 activated a subset of

87 viral genes that were different than those activated by Rta (27). Nevertheless, a broader review of the
88 literature shows that our understanding of Notch's role in KSHV reactivation remains debatable. One
89 study concluded that ectopic NICD1 is capable of inducing complete reactivation (30) by directly
90 activating Rta's promoter and a second study indicated that Notch inhibits reactivation in neighboring
91 cells by indirectly repressing Rta expression (31). The interpretation of experiments intended to analyze
92 the role of Notch signaling in KSHV reactivation are complicated by two observations: first, Notch
93 signaling is constitutively-active in all KSHV-infected cells, and second, one or more of the activated
94 Notch proteins (i.e. NICD1-4) is required for growth and survival of KSHV-infected cells (29, 32-38).
95 Indeed, Notch isoforms 1, 2, and 4, Notch activating ligands, and numerous Notch target genes are
96 overexpressed and active in KS lesional tissue, PEL cells, and in KSHV-infected endothelial cells.
97 Notch signaling is also reciprocally impacted by KSHV infection in myriad and complex ways.
98 The expression of Notch ligands and receptors are increased by specific latent and lytic viral proteins,
99 including Rta, in infected lymphatic endothelial cells (29, 33, 35-37). Notch signaling is reprogramed
100 when the viral immediate early protein Rta stimulates RBP-Jk DNA binding and by proteolytic
101 processing of Notch effector proteins (4, 7, 26, 39). Rta-dependent stimulation of RBP-Jk binding to the
102 KSHV Mta promoter converts it to a Notch-responsive gene (4). Moreover, our ChIP/Seq studies
103 demonstrated that RBP-Jk binding to the viral genome is dramatically redistributed during reactivation,
104 but Rta and RBP-Jk do not co-occupy every newly identified RBP-Jk site (26). Taken together, these
105 data suggest that Notch plays an essential and complementary role with Rta in KSHV reactivation.
106 While it is clear that Rta is the only viral protein that is necessary and sufficient to reactivate the
107 complete KSHV lytic cycle, a complete understanding of Rta's reactivation function must consider the
108 intracellular environment that is replete with potent, constitutive Notch activity.
109 In the present study, we use the KSHV-infected Vero cell model and multiple complementary
110 methodologies to demonstrate that Notch signaling is key to viral reactivation. Specifically, we

111 demonstrate that exposing infected cells to the Notch small-molecule-inhibitor DAPT, or to Notch-
112 inhibiting dominant negative Mastermind-like (dmMAML)-1, severely reduces production of infectious
113 KSHV. Reactivation reduction occurs after either chemical induction of virus or forced expression of
114 Rta. Inhibition of KSHV virion production is accompanied by reduction of selected viral transcripts and
115 proteins. Importantly, reactivation stymied by DAPT treatment is not the result of cell growth reduction
116 by the drug. While we show that none of the four Notch isoforms are sufficient to reactivate the virus,
117 transfection of specific siRNAs implicates Notch 1 as one of the isoforms that contribute to Rta-induced
118 reactivation. Finally, we also observe a block in reactivation, which is measured here by a decrease in
119 viral DNA production, by inhibiting Notch in naturally KSHV-infected PEL cells. Taken together, our
120 study illustrates that although Rta is necessary and sufficient for KSHV reactivation, viral reactivation
121 relies on continued endogenous Notch signaling, likely by working with Rta cooperatively during the
122 early steps of reactivation.
123
124
125

126 **Materials and Methods**

127

128 **Plasmids:** All plasmids were grown in DH5α *E. coli* and purified using the cesium chloride maxi-prep
129 method (40). All prepared plasmids were confirmed via restriction enzyme digestion and/or sequencing.
130 pcDNA3-FLg50 expresses full length Rta protein from a genomic allele of KSHV ORF50 (41).
131 pCAGGS:dnMAML1-GFP and pEGFP-N1-dnMAML1 express dominant negative mutants of MAML1
132 fused to GFP and were gifts of Dr. Signe V. Horn Pederson (42). pEGFP-N1-H2b (referred to as H2b-
133 GFP) expresses GFP-fused histone H2b and was a gift of Dr. Geoff Wahl (Addgene plasmid #11680)
134 (43). pcDNA3.1-HisLacZ (11) expresses β-galactosidase reporter protein under control of the HCMV
135 enhancer. The reporter plasmids 4xCSL-luciferase (Addgene plasmid #41726) and 4xCBS-luciferase
136 encode firefly luciferase under the control of four RBP-Jk binding sites are were gifts of Dr. Raphael
137 Kopan and Dr. Rhett Kovall, respectively (44, 45). p3xFLAG-NICD 1-4 express Notch intracellular
138 domains (NICD) 1-4 from the p3xFLAG-CMV-7 expression vector and were gifts of Dr. Raphael
139 Kopan (46). pcDNA3.1-ORF50ΔSTADV5 expresses transcriptionally inert, dominant negative KSHV
140 Rta (nts 1-1590) fused to the V5 epitope tag (11). pCMV-NICDΔPEST, NICD1-P12, NICD1-L1594P
141 express NICD1 alleles containing different activating mutations found in human T cell acute
142 lymphoblastic leukemia lymphoma cells provided by Dr. Jon C. Aster (47). pcDNA3 (Invitrogen) was
143 used as an empty vector control ("Vec") and DNA filler for all experiments.

144

145 **Cell Culture:** 293 MSR-tet OFF and Vero rKSHV.294 cells (gifts of Dr. Jeff Vieira) were maintained
146 as previously described (28, 48). BC3 cells (a gift of Dr. Ethel Cesarman) and BCBL-1 cells were
147 maintained in RPMI medium supplemented with 12% or 10% Fetal Bovine Serum (FBS) respectively,
148 1% glutamine, 50uM β-mercaptoethanol, and 1% penicillin/streptomycin.
149 Viral reactivation was induced chemically by treatment of cells with 1 mM Valproic acid (VPA;

150 Sigma, P4543; prepared in dH_2O and filtered through 0.22uM surfactant-free cellulose acetate (SFCA)).
151 Notch activity was inhibited chemically by treatment of cells with (2*S*)-*N*-[(3,5-
152 Difluorophenyl)acetyl]-L-alanyl-2-phenyl]glycine 1,1-dimethylethyl ester (DAPT; Selleckchem,
153 S2215); concentrations are given in the figure legends. The solvent vehicle for DAPT was dimethyl
154 sulfoxide (DMSO), which was used as the control, vehicle ("Vh") treatment in all experiments.
155
156
157 **Transfections:** Vero rKSHV.294 cells were plated at a concentration of $2x10^5$ cells per well of 6-well
158 plates and incubated at 37°C overnight. The following day, 2.5 ug of total plasmid DNA and 5 uL of
159 vortexed TransIT-LT1 reagent were added to 250 uL incomplete DMEM and incubated at RT for 30m.
160 The mixture was added to the Vero rKSHV.294 cells dropwise, and cells were incubated for 48 or 72h at
161 37°C, for protein harvest or SeAP assay respectively. Specific plasmids used in transfections are
162 indicated in respective figure legends.
163 For siRNAs, Vero rKSHV.294 cells were plated at a concentration of $2x10^5$ cells per well of six-
164 well plates and incubated overnight at 37° C. The following day, 30 pmol of either control siRNA-A
165 (Santa Cruz, sc-37007), Notch 1 siRNA (h) A (Santa Cruz, sc36095A), or Notch 1 siRNA (h2) (Santa
166 Cruz, sc-44226A) were diluted in 150 uL of incomplete DMEM and mixed with 9 uL of Lipofectamine
167 RNAiMAX reagent previously diluted in incomplete DMEM per manufacturers' suggestions. The
168 mixtures were incubated for 5m at RT, then added to cells.
169
170 **Secreted Alkaline Phosphatase (SeAP) Assay:** Virus-containing media from Vero rKSHV.294 cells
171 were transferred to 293 MSR-tet-OFF cells previously plated at a density of $2x10^5$ cells/well in 6-well
172 plates 24h earlier. 293 MSR-tet-OFF cells were returned to the incubator for 72h (unless otherwise
173 indicated) at 37°C. SeAP-containing media were harvested, and 20 or 25 uL were assayed using either
174 the Great EscAPe SeAP kit (Takara/Clontech) or the Phospha-Light System (Applied Biosystems).

175

176 **Protein extractions and assays**: Cells were washed with 1x PBS, and lysed using RIPA buffer (150
177 mM NaCl, 1% NP40, 0.5% sodium deoxycholate, 0.1% SDS, 50 mM Tris pH 8.0) supplemented with
178 protease inhibitor cocktail (Sigma P2714) and 1 mM DTT. Dishes were scraped, contents were
179 transferred to microfuge tubes, debris was pelleted by centrifugation, and supernatants were transferred
180 to new microfuge tubes. Total protein concentrations were determined by Protein Assay (Bradford; Bio-
181 Rad).

182 For luciferase and β-galactosidase quantitation, at 48h post-transfection, cells were washed twice
183 with 1x PBS, then lysed in 125 uL 1x reporter lysis buffer (Promega) for 20min at RT. Dishes were
184 scraped, contents were transferred to microfuge tubes, debris was pelleted by centrifugation, and
185 supernatants were transferred to new microfuge tubes. Luciferase activity was measured in the BD
186 monolight 3010 luminometer (BD Biosciences) using 20 uL of each extract into which 20 uL luciferase
187 assay substrate was injected (Promega). β-galactosidase activity was measured by absorbance at 420 nm
188 in the Tecan Genios plate reader using 30 uL of each extract mixed with 30 uL of 2x Assay Buffer
189 (Promega).

190

191 **SDS-PAGE and Western Blotting:** Protein samples were mixed with 6x Laemmli buffer containing
192 freshly added β-mercaptoethanol, heated at 95°C for 5m, then loaded on gels. Proteins were transferred
193 via electroblotting to nitrocellulose (Main Manufacturing LLC) or PVDF (GVS Filter Tech 1212783;
194 PVDF membranes only were initially dipped in 100% methanol). Membranes were blocked with 5%
195 milk in 1x PBS/0.1% Tween 20 (blocking buffer) for at least 30m, then washed with 1x PBS/0.1%
196 Tween 20 and 1x PBS. Primary antibodies were diluted in blocking buffer then incubated with the blots
197 for 4h at RT or overnight at 4°C; antibodies and dilutions were as follows: anti-Notch1 (1:200, Santa
198 Cruz sc-32745, or bTAN20 Developmental Studies Hybridoma Bank, deposited by Dr. Spyros

199 Artavanis-Tsakonas), anti-Rta (1:4000, D3861 (12)), anti-FLAG (1:1000, M2 Sigma Aldrich F1804, or
200 PA1-984B Thermo scientific), anti-GAPDH (1:1000, BioLegend 919501), anti-GFP (1:200, B-2 Santa
201 Cruz sc-9996) anti-ORF59 (1H10; (12)), anti-KbZIP (49) or anti-Mta (50). The membranes were then
202 washed with 1x PBS/0.1% Tween 20 and 1x PBS and incubated for 30m with secondary antibodies
203 diluted in blocking buffer; antibodies and dilutions were as follows: Goat anti-Mouse IgG-h+1 HRP
204 conjugated (1:5000, Bethyl Labs A90-116P), Rabbit TruBlot anti-Rabbit IgG (1:1000, Rockland 18-
205 8816-33), Goat anti-Rabbit IgG-h+1 HRP conjugated (1:5000, Bethyl A120-101P). Membranes were
206 partially dried and incubated for up to 2m in Pierce ECL Western Blotting Substrate (Thermo Scientific,
207 32016). Signals were detected by exposure to autoradiography film (Denville, E3012) for up to 24h, or
208 digitally captured using myECL imager (Thermo Scientific) or Chemidoc (BioRad).
209
210 **Quantitative Reverse Transcription-real-time Polymerase Chain Reaction (RT-qPCR)** Total RNA
211 was extracted from Vero rKSHV.294 cells using the RNeasy kit (Qiagen) as per manufacturer's
212 suggestions. DNA contamination was removed using the TURBO DNA-free kit (Invitrogen) as per
213 manufacturer's suggestions. Transcripts were quantitated by qRT-PCR using the iTaq Universal SYBR
214 Green One-Step Kit (Bio-Rad) following manufacturer's suggestions. 5 to 100 ng. of input RNA was
215 amplified using KSHV-specific unique coding sequence primers (51) or β-actin primers (52) in a
216 CFX96/C1000 instrument (Bio-Rad). Reaction conditions were 10 mins 50ºC for RT, 1 min 95ºC, then
217 40 cycles of 10 sec 95ºC/10 sec 60ºC. Amplification specificity was confirmed for all primer pairs by
218 melt-curve analysis and parallel control reactions that lacked template RNA or reverse transcriptase.
219
220 **vDNA quantitation:** BC3 cells were treated with indicated chemicals for 65h and total DNA was
221 purified from cell lysates using the FlexiGene DNA kit (Qiagen). Intracellular viral DNA was measured
222 by real-time quantitative (q) PCR of the viral genome; GAPDH was the internal control. qPCR reactions

223 were performed using SYBR Green PCR Master Mix (Thermo Scientific). Input DNA (100 ng) was
224 amplified by incubating at 50°C for 10m and 95°C for 10m, then cycled 39 times with melting at 95°C
225 for 15 sec and annealing at 60°C for 1m. Fold DNA was calculated using the ΔCt method and all values
226 were normalized to that of VPA + vehicle, which was set to 100%.
227
228 **Immunofluorescence**: Cells were harvested in 15 mL conical tubes, washed twice with 1x Phosphate
229 Buffered Saline (PBS), and resuspended at a density of $1.25x10^6$ cells/mL in 1x PBS. 15-20 mm circles
230 were drawn on glass microscope slides with a Super PAP pen (ThermoFisher 008899), then coated by a
231 10m incubation with 4 uL poly-L-lysine. Polylysine was removed, 200 uL of cells/circle were adhered
232 for 30m, then fixed in pre-chilled methanol/acetone (50/50 v/v) at -20°C for 5 to 10min. Slides were air
233 dried for 10min at RT and cells were blocked with 3% BSA/1% glycine in 1x PBS. The following
234 primary antibodies were diluted in 1:1000 in blocking buffer and incubated for 1h with the cells: anti-
235 Rta (D3861; (12)), anti-K8.1 (Santa Cruz Bio sc-65446, 1:1000), or anti-ORF59 (1H10; (12)). Cells
236 were washed with 1x PBS/0.4% Tween20 and 1x PBS, then the following secondary antibodies were
237 diluted 1:500 in blocking buffer and incubated for 1h with the cells: anti-rabbit DyLight 448 (Thermo
238 Scientific, 35552), anti-rabbit DyLight 550 (Thermo Scientific, 84541), or anti-mouse DyLight 550
239 (Thermo Scientific, 84540). Cells were re-washed, and coverslips were mounted to slides using Vecta-
240 shield with DAPI (Vector Labs).
241
242 **Cell Growth Quantitation:** Vero rKSHV.294 cells were plated at a density of 6.7×10^3 cells/well of a
243 96-well dish. 24 h later, cells were treated with 1 uL vehicle alone (control) or containing DAPT (final
244 concentration of 1 or 5 uM), in triplicate. Three mock wells were also prepared with media only for
245 each time point. At the post-treatment times indicated, cell media was replaced with 200 uL growth
246 assay media (180 uL DME + 20 uL Alamar Blue (BioRad BUF012A), and incubation was continued for

247 4 hr at 37°C. Alamar Blue fluorescence was measured by excitation at 544 nm/emission at 590 nm in a
248 SpectraMax M2 plate reader (Molecular Devices). Mock values were averaged and subtracted from
249 each experimental value to yield corrected values. All corrected values were then normalized to 0h
250 values that had been set to the relative value of 1 for each treatment.

251

252

253

254 **Results**

255 **Notch1 is constitutively active in KSHV-infected Vero cells**

256 To understand the complex interactions of Notch signaling with KSHV infection, we have
257 employed an infected Vero cell model. These cells have emerged as a robust system for understanding
258 host and viral regulation of productive KSHV reactivation. Infected Vero cells provide a number of
259 improvements over other reactivation models, including their ease of transfection. Gantt and colleagues
260 (48) developed a Vero cell line that produces a recombinant KSHV reporter virus upon reactivation that
261 is quantifiable by infecting a trans-complementing 293 cell line. Using this system, we previously
262 demonstrated that ectopic, activated Notch1 (NICD1) was insufficient to produce infectious virus,
263 confirming work from studies of PEL cells (4, 27, 28).

264 Many cellular models of KSHV infection demonstrate constitutive activation of NICD1 (29, 32,
265 34-36) which is required to maintain cell growth and survival (34-36). Based on the dramatic
266 association of Notch activity with KSHV infection in those cells, we sought to determine the status of
267 Notch1 in infected Vero cells. We prepared total protein extracts from infected Vero cells that were
268 grown for 24h. Western blotting with anti-Notch1-specific antisera demonstrated a protein band doublet
269 that migrated with an apparent molecular weight (MW) of 100-120 kDa (Fig. 1). The doublet matched
270 the pattern and migration of the bands observed from control, uninfected Vero cells transfected with an
271 NICD1 expression vector (Fig. 1 "Con"). Therefore, we conclude that Notch1 is constitutively active in
272 latent, KSHV-infected Vero cells. Others have shown that expression of one or several productive cycle
273 KSHV proteins could induce expression of Notch pathway components in 293 cells (37). However, we
274 found that treating the infected Vero cells with VPA to reactivate the virus had no effect on the
275 constitutively high amount of NICD1 in the cells (not shown).

276

277
278

279 **Inhibiting Notch activation reduces KSHV reactivation**

280 To determine whether endogenous, constitutive Notch activity contributed to KSHV reactivation,
281 we measured the effect of DAPT treatment on mature infectious virus production from Vero
282 rKSHV.294 cells. Cells were pre-treated with DAPT or the vehicle control ("Vh"; DMSO) for 24h, then
283 transfected with Rta expression vector to induce viral reactivation or empty vector (Vec) control. When
284 Notch is active, which is the case in the Vh only cultures, ectopic Rta reactivates virus to approximately
285 700-fold greater than Vec, as we previously published (Fig. 2A) (28). In cells where Notch is inhibited,
286 which is the case in the DAPT-treated cells, and viral reactivation is attempted by Rta addition,
287 reactivation is stymied. These data suggest that constitutive Notch activity is necessary for optimal viral
288 growth (Fig. 2A).

289 Since reactivation is scored by transferring the supernatants from the infected Vero cells to 293
290 MSR tet-OFF cells, we performed a key control experiment to assess the potential effect of DAPT on
291 the function of the 293 reporter cells. We treated virus-containing supernatant media from the
292 experimental Vero rKSHV.294 cells with DAPT prior to incubating the supernatants with the 293 cells.
293 There was no decrease in virus detection in the 293 cells, confirming that DAPT does not inhibit *de*
294 *novo* infection by KSHV nor expression of the SEAP reporter protein (not shown).

295 To confirm that NICD activity was reduced by DAPT treatment in the infected Vero cells, we co-
296 transfected the Vero rKSHV.294 cells with two reporter plasmids. One contained four RBP-Jk motifs
297 arrayed in tandem upstream of a luciferase reporter gene, and the other contained the HCMV enhancer
298 sequence lacking RBP-Jk motifs for normalization. As expected, treatment of the cells with 5 uM
299 DAPT for 6 or 24h reduced Notch activity relative to vehicle-treated cells (Fig. 2B).

300

301 **Inhibiting Notch activation does not reduce growth of KSHV-infected Vero cells**

302 Notch inhibition by DAPT can inhibit growth and induce apoptosis in KSHV-infected cells (29,
303 32-38). To determine the effect of DAPT on growth of the infected Vero rKSHV.294 cells, we
304 measured cell viability by alamarBlue sensitivity. Over a 72h period of growth, cells treated with 1 uM
305 or 5 uM DAPT maintained normal cell viability (Fig. 2C). The Fig. 2 data therefore support the
306 conclusion that Notch inhibition by DAPT treatment specifically reduces viral reactivation without
307 affecting Vero cell growth or viability.
308
309 **Inhibiting the Notch transactivation complex reduces KSHV reactivation**
310 Inhibiting the gamma-secretase complex with DAPT can block the formation of several signaling
311 substrates in addition to Notch (53). Therefore, we worked to specifically block Notch activity directly
312 at its site of transcriptional transactivation by testing the effects of ectopically expressing dominant
313 negative (dn) mutants of the Mastermind-like1 (MAML1) protein. Cognate MAML1 stabilizes the
314 NICD1/RBP-Jk/DNA complex to facilitate NICD1-dependent transactivation in the nucleus (54, 55).
315 Transfection of Vero rKSHV.294 cells with two different dnMAML1 expression vectors reduced Rta-
316 mediated reactivation by 40% or 90%, respectively (Fig. 3A). As a control, we observed that dnMAML1
317 proteins were strongly expressed (Fig 3B).
318 To determine if viral gene expression was similarly debilitated by inhibiting the Notch
319 transactivation complex during reactivation, we measured protein and transcript levels in the infected
320 Vero cells. We observed a gene specific reduction in viral proteins (Figs 3C and D) and RNAs (Fig 3E)
321 in cells expressing dnMAML1 relative to empty vector-transfected cells. The expression of Mta, KbZIP,
322 K2, and K8.1 proteins and transcripts were significantly reduced by inhibiting Notch transactivation
323 with dnMAML1. We conclude that activated Notch supports production of infectious KSHV by
324 transactivating specific, essential viral genes in cooperation with Rta.
325

326 **Notch1 is necessary for optimal viral reactivation**
327

328 The data in Figs. 2 and 3 show that inhibiting Notch post-translationally at two different
329 biochemical steps of its activation dramatically reduced KSHV reactivation and support a pro-viral role
330 for Notch signaling in viral reactivation in Vero cells. However, these experiments do not specify which
331 of the four Notch receptors, Notch1,2,3 or 4, are required for efficient reactivation, as all four proteins
332 are inhibited by DAPT and ectopic dnMAML1 (2, 54, 56-60).
333 Since Notch1 is constitutively active in Vero cells, we asked whether specific knock-down of
334 Notch1 would affect viral reactivation. We transfected two different siRNAs to knock-down
335 endogenous Notch1 in Vero-rKSHV.294 cells, and then induced viral reactivation by transfection of Rta
336 expression vector (Fig. 4A) or VPA treatment (Fig. 4B). The Notch1-specific siRNAs reduced viral
337 reactivation in all cases relative to control, scrambled siRNA ("Scr"), up to a maximum of ~80%
338 inhibition ("N1-B" in Fig. 4A). Knock-down of endogenous Notch1 was confirmed via Western blot
339 (Fig 4C). These data verify that constitutively active Notch1 plays a pro-viral role in KSHV reactivation
340 in Vero cells.
341
342
343 **Notch is pro-viral in PEL cells**
344
345 Notch1 is constitutively active in PEL cells (34-36). To determine whether Notch1 also supports
346 reactivation in these cells, we reactivated virus with VPA in the presence of 16, 32, or 40 uM of DAPT
347 and quantitated vDNA accumulation and protein expression. DAPT reduced intracellular vDNA
348 accumulation up to a maximum of ~80% relative to VPA plus vehicle control ("Vh") (Fig 5A). DAPT
349 also reduced the percentage of K8.1-positive cells (Fig. 5B); as K8.1 is a true-late gene, this result was
350 consistent with the effect of DAPT on vDNA accumulation. Interestingly, we did not observe an effect
351 of DAPT treatment on the percentage of ORF59-positive cells, perhaps because our assay was not
352 designed to detect modest effects on the ORF59 amounts or signal intensity (Fig 5B).

353 In an SLK cell model of KSHV infection, Notch was shown to inhibit reactivation and reduce
354 expression of productive cycle genes, including Rta (31). In contrast, we did not observe a statistically
355 significant effect of DAPT treatment on Rta expression in any of the experiments we performed in
356 Vero and PEL cells (not shown).
357

358 **Ectopic, activated Notch isoforms 1 to 4 are insufficient to reactivate KSHV from latency**

359 In our experiments using the infected Vero cell system, as well as experiments in PEL cells, we
360 demonstrated that ectopic NICD1 is incapable of productively reactivating KSHV, despite widespread
361 RBP-Jk binding to the latent viral genome (4, 7, 28). Although other Notch isoforms are commonly
362 constitutively-expressed in KSHV-infected cells (29, 32, 34-36) it is possible that their endogenous
363 levels are insufficient to drive viral reactivation. To test whether ectopic Notch isoforms 2, 3, and 4
364 could reactivate KSHV, we transfected vectors that express NICD 2, 3, and 4 into Vero rKSHV.294
365 cells. As expected, ectopic Rta, the positive control, gave a 500-fold increase in KSHV reactivation as
366 measured by SeAP activity (Fig. 6A). However, little to no virus was detectable from cells transfected
367 with any of the NICD expression vectors (NICD1, 1.1-fold; NICD2, 9.4-fold; NICD3, 2.9-fold; NICD4,
368 4.8-fold), similar to effects in cells transfected with the Rta transcriptionally deficient mutant
369 ORF50ΔSTAD (1.7-fold; Fig. 6A). All four isoforms were thus insufficient to reactivate KSHV from
370 Vero cells, despite their robust expression levels (Fig 6B).
371

372 **Ectopic NICD1 and 2 are transactivation competent in KSHV-infected Vero cells**

373 It is possible that the activated Notch proteins are unable to reactivate KSHV because they are not
374 transcriptionally active in Vero rKSHV.294 cells. To assess their activities, we co-transfected Vero
375 rKSHV.294 cells with a reporter vector containing four tandem RBP-Jκ sites, and each of the four NICD
376 expression vectors at the same amounts as in Fig 6. We observed significant transactivation of this

377 promoter by both NICD1 and 2, but not NICD3 or 4 (Fig 7). Taken together with Fig. 6, these data
378 confirm that NICD1 and 2 are incapable of reactivating KSHV despite being transcriptionally active.
379 However, the inability of NICD3 or 4 to activate transcription in these cells provides a potential
380 explanation for their inability to reactivate KSHV from latency.
381
382 **NICD mutants of varying activity are insufficient to reactivate KSHV from latency**
383 To determine whether varying the potency of ectopic, activated NICD1 could reactivate KSHV,
384 we tested a series of constitutively-active Notch alleles with varying intrinsic signaling strengths that
385 had been cloned from clinical T cell acute lymphoblastic leukemia (T-ALL) lymphomas (47, 61). Each
386 of these Notch alleles contain distinct mutations that render the protein more stable (NICDΔPEST) or
387 promote constitutive cleavage and activation (P12 and L1594P). NICDΔPEST was classified as a very
388 weak allele as it was unable to influence hematopoiesis or induce T-ALL but was found to cooperate
389 with other T-ALL initiators, including c-myc. NICD-L1594P was classified as having weak signal
390 strength due to its ability to affect hematopoiesis, but not induce T-ALL, while NICD-P12 was
391 considered a strong mutant due to its ability to induce T-ALL. We transfected vectors expressing each
392 of these alleles into the Vero rKSHV.294 cells and found that none could reactivate the virus, similar to
393 the result with cognate NICD1 ("WT"; Fig 8). These data further verify that NICD1 is insufficient to
394 reactivate KSHV from latency, regardless of its potency.
395
396 **NICD1 cooperates with VPA in reactivation**
397 Our data showed that endogenous Notch1 is constitutively active in infected Vero cells and
398 supports optimal viral reactivation that is induced by VPA treatment or by ectopic Rta expression.
399 However, increasing activated Notch1 amounts alone, via ectopic NICD1 expression, was insufficient to
400 productively reactivate KSHV. To determine whether ectopic NICD1 could cooperate with VPA

401 treatment, we transfected the Vero rKSHV.294 cells with the NICD1 expression vector alone or with 1
402 mM VPA treatment. In positive control samples treated with VPA alone, we observe approximately
403 350-fold reactivation (Fig 9). As expected, ectopic expression of NICD1 alone was insufficient to
404 produce virus (Fig 9). However, expression of ectopic NICD1 in VPA-treated cells enhanced
405 reactivation to about 700-fold (Fig 9), supporting a cooperative role for NICD1 and VPA.
406
407

408 **Discussion**

409 In this work, we demonstrate that ectopic expression of activated Notch1 is insufficient to
410 productively reactivate KSHV from latency (Fig 6). NICD1's reactivation insufficiency confirms our
411 earlier results from ectopic expression of NICD1 in PEL and Vero cells (4, 28), and agrees with similar
412 results in which NICD1 was conditionally-induced ectopically in a stably-transfected PEL cell line (27).
413 To ensure that this negative result is not due to an inadequate dose of ectopic NICD1, we show that three
414 additional Notch1 alleles that encode constitutively active NICD1 proteins with varied intrinsic
415 transcriptional potency also fail to reactivate KSHV from latency (Fig 8). Our work is the first to test all
416 four of the NICD isoforms in this capacity, and conclusively establishes that ectopic NICD2 is also not
417 capable of reactivating the virus. While ectopic expression of NICD isoforms 3 and 4 also did not result
418 in production of infectious virus, we are unable to conclude that NICD3 and 4 are similarly insufficient
419 to reactivate KSHV since we could not determine that they are transcriptionally active in our
420 experiments (Fig 7). However, since the Notch isoforms have been shown to have different promoter
421 transactivation specificities (46, 62-64), it is possible that NICD3 and 4 are, in fact, active in Vero cells,
422 but are simply incapable of activating the 4x tandem RBP-Jk motif (4x CBS) reporter plasmid. NICD1
423 and 2 have been suggested to be functionally interchangeable in other biologic systems (65-67).

424 Despite Notch's inability to reactivate latent KSHV alone, we show that constitutive Notch1
425 activity is required for robust reactivation of the virus. All three of our strategies that inhibited

426 endogenous Notch activity in the Vero cells decreased Rta or VPA-induced reactivation over a range of
427 60-90% (Figs 2 to 5). Two of the strategies, DAPT treatment and dnMAML1 expression, are well-
428 established strategies to broadly inhibit all four Notch isoforms (2, 54, 56-60). DAPT blocks gamma-
429 secretase activation of endogenous Notch and dnMAML1 interferes with the formation of Notch
430 transactivation complexes (44, 68-70). However, neither strategy is strictly Notch-specific, because each
431 also interferes with other cellular processes that require gamma-secretase activity or cognate MAML1
432 (53, 55). To inhibit Notch1 specifically, we knocked-down its expression using two different transfected
433 siRNAs (Fig. 4). Inhibiting Notch with dnMAML1 reduced reactivation more dramatically than did
434 siRNA knock-down, suggesting that endogenous Notch 2, 3, and 4 may also have pro-viral functions
435 (compare Figs 3 and 4). Our Notch inhibition studies focused primarily on quantitating production of
436 infectious virus from latently infected Vero cells, but we also observed that inhibiting Notch in PEL
437 cells reduced synthesis of intracellular viral DNA (Fig 5). Those data suggest that Notch activity in both
438 cell lines have similar effects on viral infection. We note a single contradictory study that concluded that
439 ectopic NICD1 reactivated KSHV (30).
440 It is well-established that Notch signaling is critical for cell and animal models of KSHV
441 pathogenesis; however, our data are the first to demonstrate that Notch activation is necessary for robust
442 production of infectious virus. Productive cycle gene expression is also seen in the context of sustained
443 Notch activation that is required for the endothelial to mesenchymal transition of KSHV-infected cells
444 (29, 33, 37, 38). Growth and survival of KSHV-infected cells also depend on Notch activity:
445 proliferation rates of KSHV-infected B cells were proportional to Notch expression levels, and Notch
446 inhibition reduced cellular cyclin D1 expression and arrested cells in G1 (35). Moreover, pharmacologic
447 Notch inhibition induced apoptosis of infected SLK, B, and primary KS tumor cells (29, 32, 33, 35-38)
448 and induced necrosis of PEL xenografts in NOD/SCID mice (34). Although Notch1 expression is
449 insufficient to productively reactivate KSHV, ectopic Notch1 could induce expression of a subset of

450 productive cycle viral genes in PEL cells (27). Importantly, the infected Vero cell model used in our
451 work is ideal for uncoupling the effect of Notch on cell growth from its effect on viral reactivation; in
452 our work, we used DAPT concentrations that significantly reduced production of infectious virus
453 without affecting host cell doubling time or survival (Fig 2C). This pro-viral role of Notch follows the
454 paradigm established in foundational tumor virus studies in which cellular oncogenic pathways
455 manipulated by SV40 or Adenovirus also support productive viral infections (71).

456 Our data raise two intriguing questions: how does activated Notch contribute to reactivation and
457 why is it not sufficient to reactivate KSHV alone? Since complete Notch ablation is inconsistent with
458 survival of KSHV-infected cells, one apparent contribution of activated Notch is to maintain survival of
459 cells in which KSHV is reactivating (29, 32, 34-38). To this end, we note that none of our strategies to
460 reduce Notch activity were 100% effective in debilitating virus production. However, our observation
461 that DAPT treatment and partial NICD1 knock-down can debilitate reactivation without reducing cell
462 growth suggests a function of Notch that is complementary to Rta and independent of cell survival. Our
463 data also show that NICD1 is transactivation competent in latently-infected Vero cells (Fig 7), as has
464 also been demonstrated in latently-infected PEL cells (27). Thus, all of the components sufficient to
465 form the Notch1 transactivation complex must be expressed and functional in KSHV-infected cells
466 (reviewed in (2, 3, 72)). Therefore, we believe that Notch's insufficiency to reactivate KSHV derives
467 from a limit to gene-specific transactivation that is relieved when Rta is expressed. Importantly, one
468 critical gene which ectopic NICD1 fails to activate in Vero and PEL cells is Rta (data not shown; (27)).
469 Therefore, when endogenous Rta is induced by VPA, or Rta is expressed ectopically, endogenous
470 NICD1 then likely transactivates specific viral genes during reactivation. This hypothesis for gene-
471 specific transactivation by NICD1 is supported by the different sensitivities of expression of the viral
472 genes Mta, KbZIP, K2, K8.1 and ORF59 observed in response to Notch inhibition (Fig. 3C to E and Fig
473 5B). Our observation that broad Notch inhibitors have greater anti-viral potency than specific Notch1

474 inhibition (compare Figs 2A and 3A to Fig 4A) suggests that at least one additional Notch isoform also
475 supports optimal KSHV reactivation.

476 We interpret our data as revealing that Notch activity had no influence on productive reactivation
477 unless Rta was expressed. Activated Notch has no intrinsic DNA binding ability, but instead relies upon
478 the cellular DNA binding protein RBP-Jk to specify NICD1's target genes (2, 3, 73) . One function of
479 Rta which can profoundly influence the ability of NICD1 to transactivate specific genes is Rta's ability
480 to stimulate RBP-Jk DNA binding (4, 7, 26). Our lab modeled this mechanism by showing that NICD1
481 can transactivate the Mta promoter only if a truncated form of Rta, lacking its transactivation domain,
482 stimulates RBP-Jk binding to the promoter (4). Studying the intact virus, we showed that KSHV
483 reactivation is associated with dramatic re-localization of RBP-Jk to unique sites on the virus genome
484 (26). The extent of dynamic RBP-Jk binding to the virus can be contrasted with that observed on the cell
485 genome. In uninfected cells, RBP-Jk binding sites on the cellular genome are classified as static or
486 dynamic, and NICD1 can stimulate RBP-Jk DNA binding to cellular genomes (74-77). However, on the
487 KSHV genome, the proportion of dynamic RBP-Jk sites in our studies vastly exceed the proportion of
488 dynamic sites reported on cellular genomes (26, 74, 75, 78-81). In fact, the number of reactivation-
489 specific RBP-Jk sites on the virus, and the number of RBP-Jk DNA motifs on the virus, exceed the
490 number of KSHV ORFs (26). Moreover, Rta is not found bound to the virus at every RBP-Jk site (26).
491 We hypothesize that NICD1/MAML1/RBP-Jk complexes transactivate specific essential viral promoters
492 and cooperate with Rta to support KSHV reactivation (Fig 9). During latency, in the absence of Rta
493 expression, NICD1/RBP-Jk fails to form a competent transactivation complex on at least one essential
494 viral promoter. Unlike NICD1, Rta also binds DNA independent of RBP-Jk for transactivation and
495 replication (82-85); these mechanistic differences probably also contribute to Notch's insufficiency in
496 reactivation.

497 Based on experimental data, we have published two mechanisms that describe how Rta regulates
498 RBP-Jk DNA binding: (1) Rta directly binds to RBP-Jk, and (2) Rta induces expression of additional
499 cellular proteins during reactivation which in turn bind to DNA adjacent to RBP-Jk (4, 7, 25, 26). The
500 latter mechanism is consistent with our work and others that demonstrated that *de novo* gene expression
501 downstream of Rta is required for robust reactivation (25, 86). Thus, NICD1 transactivation in KSHV-
502 infected cells is determined by the fate of the infection (latent vs. reactivating) and intracellular context,
503 as well as the DNA context of individual RBP-Jk binding sites. Similar context-dependent determinants
504 have been invoked to explain cell-specific variations in NICD1 transactivation and phenotypic
505 consequences in uninfected cells (46, 81, 87-96). The influence of cellular context on Notch function
506 includes interactions between the four Notch isoforms, including competition, cooperation, or
507 redundancy (63, 65, 66, 97-110).

508 In Notch cancer biology, cell context is a major determinant of the striking observation that
509 Notch can be either tumor suppressive or oncogenic in different malignancies (reviewed in (2, 111-113).
510 The ideal DNA context for an NICD1-responsive RBP-Jk site is a head-to-head configuration with a
511 second RBP-Jk site spaced 15-17 nts apart (114-117); remarkably, only six pairs of RBP-Jk motifs in the
512 KSHV genome are found in that DNA context (not shown). It is likely that the mechanisms underlying
513 contextual variations in Notch signaling outcomes in uninfected cells are functionally similar in KSHV
514 infection, but uniquely regulated by KSHV proteins like Rta. Moreover, cell context may be responsible
515 for the discordance of our observations with a publication that showed that NICD1 inhibits KSHV
516 reactivation in SLK cells (31).

517 In summary, herein we demonstrate the significance of constitutive Notch1 activity in the
518 cellular context of productive KSHV reactivation. The essentiality of Rta/RBP-Jk/DNA complexes in
519 driving reactivation is well-established, but this current study highlights the likelihood that Notch
520 contributes to reactivation by forming promoter-specific NICD1/RBP-Jk/DNA complexes, also. The

521 KSHV genome contains >100 RBP-Jk motifs of varying sequence found in varying DNA contexts that
522 we expect to respond differently to Rta and/or NICD1 to determine the success of a reactivation signal
523 leading to virus production. Moreover, our data indicate that Notch isoforms other than the well-studied
524 Notch1 may help regulate viral infection. This diversity in the molecular players underlies the
525 consequences of RBP-Jk-dependent gene expression in KSHV infection and host cell pathology.
526 Our data are consistent with the idea that the Notch-dependance of viral reactivation is a complex
527 network that, when revealed, will provide important new insights into Notch-dependent signaling in
528 mammalian cells.
529

530 **Acknowledgements**
531 We gratefully thank Drs. Jeff Vieira, Ethel Cesarman, Signe V. Horn Pederson, Geoff Wahl , Rhett
532 Kovall, Raphael Kopan, Jon C. Aster, and Spyros Artavanis-Tsakonas for cells, antibody, and plasmids.
533 The work was supported by NIH Grants AI117127 and AI150230
534
535 **References**

536 1. Watanabe T, Sugimoto A, Hosokawa K, Fujimuro M. 2018. Signal Transduction Pathways
537 Associated with KSHV-Related Tumors. Adv Exp Med Biol 1045:321-355.
538 2. Aster JC, Pear WS, Blacklow SC. 2017. The Varied Roles of Notch in Cancer. Annu Rev Pathol
539 12:245-275.
540 3. Giaimo BD, Gagliani EK, Kovall RA, Borggrefe T. 2021. Transcription Factor RBPJ as a
541 Molecular Switch in Regulating the Notch Response, p 9-30. *In* Reichrath J, Reichrath S (ed),
542 Notch Signaling in Embryology and Cancer: Notch Signaling in Cancer doi:10.1007/978-3-030-
543 55031-8_2. Springer International Publishing, Cham.

544 4. Carroll KD, Bu W, Palmeri D, Spadavecchia S, Lynch SJ, Marras SA, Tyagi S, Lukac DM. 2006.
545 Kaposi's Sarcoma-associated herpesvirus lytic switch protein stimulates DNA binding of RBP-
546 Jk/CSL to activate the Notch pathway. J Virol 80:9697-709.
547 5. Liang Y, Chang J, Lynch S, Lukac DM, Ganem D. 2002. The lytic switch protein of KSHV
548 activates gene expression via functional interaction with RBP-Jk, the target of the Notch signaling
549 pathway. Genes Dev 16:1977-89.
550 6. Liang Y, Ganem D. 2003. Lytic but not latent infection by Kaposi's sarcoma-associated
551 herpesvirus requires host CSL protein, the mediator of Notch signaling. Proc Natl Acad Sci U S A
552 100:8490-5.
553 7. Palmeri D, Carroll KD, Gonzalez-Lopez O, Lukac DM. 2011. Kaposi's sarcoma-associated
554 herpesvirus Rta tetramers make high-affinity interactions with repetitive DNA elements in the Mta
555 promoter to stimulate DNA binding of RBP-Jk/CSL. J Virol 85:11901-15.
556 8. Hilton IB, Dittmer DP. 2012. Quantitative analysis of the bidirectional viral G-protein-coupled
557 receptor and lytic latency-associated nuclear antigen promoter of Kaposi's sarcoma-associated
558 herpesvirus. J Virol 86:9683-95.
559 9. Bu W, Carroll KD, Palmeri D, Lukac DM. 2007. The Kaposi's Sarcoma-associated
560 Herpesvirus/Human herpesvirus-8 ORF50/Rta Lytic Switch Protein Functions as a Tetramer. J
561 Virol 81:5788-5806.
562 10. Lukac D, Garibyan L, Kirshner J, Palmeri D, Ganem D. 2001. DNA binding by the Kaposi's
563 sarcoma-associated herpesvirus lytic switch protein is necessary for transcriptional activation of
564 two viral delayed early promoters. J Virol 75:6786-99.
565 11. Lukac DM, Kirshner JR, Ganem D. 1999. Transcriptional activation by the product of open
566 reading frame 50 of Kaposi's sarcoma-associated herpesvirus is required for lytic viral reactivation
567 in B cells. J Virol 73:9348-61.

568 12. Lukac DM, Renne R, Kirshner JR, Ganem D. 1998. Reactivation of Kaposi's sarcoma-associated
569 herpesvirus infection from latency by expression of the ORF 50 transactivator, a homolog of the
570 EBV R protein. Virology 252:304-312.
571 13. Wang Y, Yuan Y. 2006. Essential role of RBP-Jkappa in activation of the K8 delayed-early
572 promoter of Kaposi's sarcoma-associated herpesvirus by ORF50/RTA. Virology.
573 14. Persson LM, Wilson AC. 2010. Wide-scale use of Notch signaling factor CSL/RBP-Jkappa in
574 RTA-mediated activation of Kaposi's sarcoma-associated herpesvirus lytic genes. J Virol 84:1334-
575 47.
576 15. Scholz BA, Harth-Hertle ML, Malterer G, Haas J, Ellwart J, Schulz TF, Kempkes B. 2013.
577 Abortive lytic reactivation of KSHV in CBF1/CSL deficient human B cell lines. PLoS Pathog
578 9:e1003336.
579 16. Lan K, Kuppers DA, Verma SC, Robertson ES. 2004. Kaposi's sarcoma-associated herpesvirus-
580 encoded latency-associated nuclear antigen inhibits lytic replication by targeting Rta: a potential
581 mechanism for virus-mediated control of latency. J Virol 78:6585-94.
582 17. Liu Y, Cao Y, Liang D, Gao Y, Xia T, Robertson ES, Lan K. 2008. Kaposi's sarcoma-associated
583 herpesvirus RTA activates the processivity factor ORF59 through interaction with RBP-Jkappa
584 and a cis-acting RTA responsive element. Virology 380:264-75.
585 18. Liang Y, Ganem D. 2004. RBP-J (CSL) is essential for activation of the K14/vGPCR promoter of
586 Kaposi's sarcoma-associated herpesvirus by the lytic switch protein RTA. J Virol 78:6818-26.
587 19. Chang PJ, Boonsiri J, Wang SS, Chen LY, Miller G. 2010. Binding of RBP-Jkappa (CSL) protein
588 to the promoter of the Kaposi's sarcoma-associated herpesvirus ORF47 (gL) gene is a critical but
589 not sufficient determinant of transactivation by ORF50 protein. Virology 398:38-48.

590 20. Izumiya Y, Izumiya C, Hsia D, Ellison TJ, Luciw PA, Kung HJ. 2009. NF-kappaB serves as a
591 cellular sensor of Kaposi's sarcoma-associated herpesvirus latency and negatively regulates K-Rta
592 by antagonizing the RBP-Jkappa coactivator. J Virol 83:4435-46.
593 21. Sun R, LIn SF, Gradoville L, Yuan Y, Zhu F, Miller G. 1998. A viral gene that activates lytic cycle
594 expression of Kaposi's sarcoma-associated herpesvirus. Proc Natl Acad Sci USA 95:10866-10871.
595 22. Gradoville L, Gerlach J, Grogan E, Shedd D, Nikiforow S, Metroka C, Miller G. 2000. Kaposi's
596 sarcoma-associated herpesvirus open reading frame 50/Rta protein activates the entire lytic cycle
597 in the HH-B2 primary effusion lymphoma cell line. J Virol 74:6207-6212.
598 23. Nakamura H, Lu M, Gwack Y, Souvlis J, Zeichner SL, Jung JU. 2003. Global changes in Kaposi's
599 sarcoma-associated virus gene expression patterns following expression of a tetracycline-inducible
600 Rta transactivator. J Virol 77:4205-20.
601 24. Xu Y, AuCoin DP, Huete AR, Cei SA, Hanson LJ, Pari GS. 2005. A Kaposi's sarcoma-associated
602 herpesvirus/human herpesvirus 8 ORF50 deletion mutant is defective for reactivation of latent
603 virus and DNA replication. J Virol 79:3479-87.
604 25. Bu W, Palmeri D, Krishnan R, Marin R, Aris VM, Soteropoulous P, Lukac DM. 2008.
605 Identification of Direct Transcriptional Targets of the KSHV Rta Lytic Switch Protein by
606 conditional nuclear localization. J Virol 82:10709-10723.
607 26. Gonzalez-Lopez O DJ, Goyeneche C, Mello H, Vicente-Ortiz BA, Shin HJ, Driscoll KE, Du P,
608 Palmeri D, Lukac DM. . 2019. A herpesvirus transactivator and cellular POU proteins extensively
609 regulate DNA binding of the host Notch signaling protein RBP-Jκ to the virus genome. . J Biol
610 Chem 294:13073-13092.
611 27. Chang H, Dittmer DP, Chul SY, Hong Y, Jung JU. 2005. Role of Notch signal transduction in
612 Kaposi's sarcoma-associated herpesvirus gene expression. J Virol 79:14371-82.

613 28. DeCotiis JL, Ortiz NC, Vega BA, Lukac DM. 2017. An easily transfectable cell line that produces
614 an infectious reporter virus for routine and robust quantitation of Kaposi's sarcoma-associated
615 herpesvirus reactivation. J Virol Methods 247:99-106.
616 29. Cheng F, Pekkonen P, Laurinavicius S, Sugiyama N, Henderson S, Gunther T, Rantanen V,
617 Kaivanto E, Aavikko M, Sarek G, Hautaniemi S, Biberfeld P, Aaltonen L, Grundhoff A, Boshoff
618 C, Alitalo K, Lehti K, Ojala PM. 2011. KSHV-initiated notch activation leads to membrane-type-
619 1 matrix metalloproteinase-dependent lymphatic endothelial-to-mesenchymal transition. Cell Host
620 Microbe 10:577-90.
621 30. Lan K, Murakami M, Choudhuri T, Kuppers DA, Robertson ES. 2006. Intracellular-activated
622 Notch1 can reactivate Kaposi's sarcoma-associated herpesvirus from latency. Virology 351:393-
623 403.
624 31. Li S, Hu H, He Z, Liang D, Sun R, Lan K. 2016. Fine-Tuning of the Kaposi's Sarcoma-Associated
625 Herpesvirus Life Cycle in Neighboring Cells through the RTA-JAG1-Notch Pathway. PLOS
626 Pathogens 12:e1005900.
627 32. Curry CL, Reed LL, Golde TE, Miele L, Nickoloff BJ, Foreman KE. 2005. Gamma secretase
628 inhibitor blocks Notch activation and induces apoptosis in Kaposi's sarcoma tumor cells.
629 Oncogene 24:6333-44.
630 33. Emuss V, Lagos D, Pizzey A, Gratrix F, Henderson SR, Boshoff C. 2009. KSHV manipulates
631 Notch signaling by DLL4 and JAG1 to alter cell cycle genes in lymphatic endothelia. PLoS Pathog
632 5:e1000616.
633 34. Lan K, Murakami M, Bajaj B, Kaul R, He Z, Gan R, Feldman M, Robertson ES. 2009. Inhibition
634 of KSHV-infected primary effusion lymphomas in NOD/SCID mice by gamma-secretase
635 inhibitor. Cancer Biol Ther 8:2136-43.

636 35. Lan K, Choudhuri T, Murakami M, Kuppers DA, Robertson ES. 2006. Intracellular activated
637 Notch1 is critical for proliferation of Kaposi's sarcoma-associated herpesvirus-associated B-
638 lymphoma cell lines in vitro. J Virol 80:6411-9.
639 36. Lan K, Verma SC, Murakami M, Bajaj B, Kaul R, Robertson ES. 2007. Kaposi's sarcoma
640 herpesvirus-encoded latency-associated nuclear antigen stabilizes intracellular activated Notch by
641 targeting the Sel10 protein. Proc Natl Acad Sci U S A 104:16287-92.
642 37. Liu R, Li X, Tulpule A, Zhou Y, Scehnet JS, Zhang S, Lee JS, Chaudhary PM, Jung J, Gill PS.
643 2010. KSHV-induced notch components render endothelial and mural cell characteristics and cell
644 survival. Blood 115:887-95.
645 38. Gasperini P, Espigol-Frigole G, McCormick PJ, Salvucci O, Maric D, Uldrick TS, Polizzotto MN,
646 Yarchoan R, Tosato G. 2012. Kaposi sarcoma herpesvirus promotes endothelial-to-mesenchymal
647 transition through Notch-dependent signaling. Cancer Res 72:1157-69.
648 39. Gould F, Harrison SM, Hewitt EW, Whitehouse A. 2009. Kaposi's Sarcoma-Associated
649 Herpesvirus RTA Promotes Degradation of the Hey1 Repressor Protein through the Ubiquitin
650 Proteasome Pathway. Journal of Virology 83:6727-6738.
651 40. Green MR, Sambrook J, Sambrook J. 2012. Molecular cloning : a laboratory manual, 4th ed. Cold
652 Spring Harbor Laboratory Press, Cold Spring Harbor, N.Y.
653 41. Lukac DM, Renne R, Kirshner JR, Ganem D. 1998. Reactivation of Kaposi's Sarcoma-Associated
654 Herpesvirus Infection from Latency by Expression of the ORF 50 Transactivator, a Homolog of
655 the EBV R Protein. Virology 252:304-312.
656 42. Horn S, Kobberup S, Jørgensen MC, Kalisz M, Klein T, Kageyama R, Gegg M, Lickert H, Lindner
657 J, Magnuson MA, Kong Y-Y, Serup P, Ahnfelt-Rønne J, Jensen JN. 2012. Mind bomb
658 1 is required for pancreatic β-cell formation. Proceedings of the National Academy of
659 Sciences 109:7356-7361.

660 43. Kanda T, Sullivan KF, Wahl GM. 1998. Histone-GFP fusion protein enables sensitive analysis of
661 chromosome dynamics in living mammalian cells. Curr Biol 8:377-85.
662 44. Saxena MT, Schroeter EH, Mumm JS, Kopan R. 2001. Murine Notch Homologs (N1–4)
663 Undergo Presenilin-dependent Proteolysis *. Journal of Biological Chemistry 276:40268-40273.
664 45. Yuan Z, Friedmann DR, VanderWielen BD, Collins KJ, Kovall RA. 2012. Characterization of
665 CSL (CBF-1, Su(H), Lag-1) mutants reveals differences in signaling mediated by Notch1 and
666 Notch2. J Biol Chem 287:34904-16.
667 46. Ong CT, Cheng HT, Chang LW, Ohtsuka T, Kageyama R, Stormo GD, Kopan R. 2006. Target
668 selectivity of vertebrate notch proteins. Collaboration between discrete domains and CSL-binding
669 site architecture determines activation probability. J Biol Chem 281:5106-19.
670 47. Weng AP, Ferrando AA, Lee W, Morris JPt, Silverman LB, Sanchez-Irizarry C, Blacklow SC,
671 Look AT, Aster JC. 2004. Activating mutations of NOTCH1 in human T cell acute lymphoblastic
672 leukemia. Science 306:269-71.
673 48. Gantt S, Carlsson J, Ikoma M, Gachelet E, Gray M, Geballe AP, Corey L, Casper C, Lagunoff M,
674 Vieira J. 2011. The HIV protease inhibitor nelfinavir inhibits Kaposi's sarcoma-associated
675 herpesvirus replication in vitro. Antimicrobial agents and chemotherapy 55:2696-703.
676 49. Carroll KD, Khadim F, Spadavecchia S, Palmeri D, Lukac DM. 2007. Direct interactions of
677 Kaposi's sarcoma-associated herpesvirus/human herpesvirus 8 ORF50/Rta protein with the
678 cellular protein octamer-1 and DNA are critical for specifying transactivation of a delayed-early
679 promoter and stimulating viral reactivation. J Virol 81:8451-67.
680 50. Kirshner JR, Lukac DM, Chang J, Ganem D. 2000. Kaposi's Sarcoma-Associated Herpesvirus
681 Open Reading Frame 57 Encodes a Posttranscriptional Regulator with Multiple Distinct Activities.
682 J Virol 74:3586-3597.

683 51. Bruce AG, Barcy S, DiMaio T, Gan E, Garrigues HJ, Lagunoff M, Rose TM. 2017. Quantitative
684 Analysis of the KSHV Transcriptome Following Primary Infection of Blood and Lymphatic
685 Endothelial Cells. Pathogens 6.
686 52. Journo G, Tushinsky C, Shterngas A, Avital N, Eran Y, Karpuj MV, Frenkel-Morgenstern M,
687 Shamay M. 2018. Modulation of Cellular CpG DNA Methylation by Kaposi's Sarcoma-Associated
688 Herpesvirus. J Virol 92.
689 53. Güner G, Lichtenthaler SF. 2020. The substrate repertoire of γ-secretase/presenilin. Seminars in
690 Cell & Developmental Biology 105:27-42.
691 54. Weng AP, Nam Y, Wolfe MS, Pear WS, Griffin JD, Blacklow SC, Aster JC. 2003. Growth
692 Suppression of Pre-T Acute Lymphoblastic Leukemia Cells by Inhibition of Notch Signaling.
693 Molecular and Cellular Biology 23:655-664.
694 55. Zema S, Pelullo M, Nardozza F, Felli MP, Screpanti I, Bellavia D. 2020. A Dynamic Role of
695 Mastermind-Like 1: A Journey Through the Main (Path)ways Between Development and Cancer.
696 Frontiers in Cell and Developmental Biology 8.
697 56. Maillard I, Weng AP, Carpenter AC, Rodriguez CG, Sai H, Xu L, Allman D, Aster JC, Pear WS.
698 2004. Mastermind critically regulates Notch-mediated lymphoid cell fate decisions. Blood
699 104:1696-1702.
700 57. Saravanamuthu SS, Gao CY, Zelenka PS. 2009. Notch signaling is required for lateral induction
701 of Jagged1 during FGF-induced lens fiber differentiation. Dev Biol 332:166-76.
702 58. Bagheri L, Pellati A, Rizzo P, Aquila G, Massari L, De Mattei M, Ongaro A. 2018. Notch pathway
703 is active during osteogenic differentiation of human bone marrow mesenchymal stem cells induced
704 by pulsed electromagnetic fields. J Tissue Eng Regen Med 12:304-315.
705 59. Lilly B, Kennard S. 2009. Differential gene expression in a coculture model of angiogenesis
706 reveals modulation of select pathways and a role for Notch signaling. Physiol Genomics 36:69-78.

707 60. Sastre M, Steiner H, Fuchs K, Capell A, Multhaup G, Condron MM, Teplow DB, Haass C. 2001.
708 Presenilin-dependent γ-secretase processing of β-amyloid precursor protein at a site corresponding
709 to the S3 cleavage of Notch. EMBO reports 2:835-841.
710 61. Chiang MY, Xu L, Shestova O, Histen G, L'Heureux S, Romany C, Childs ME, Gimotty PA, Aster
711 JC, Pear WS. 2008. Leukemia-associated NOTCH1 alleles are weak tumor initiators but accelerate
712 K-ras-initiated leukemia. J Clin Invest 118:3181-94.
713 62. Beatus P, Lundkvist J, Oberg C, Pedersen K, Lendahl U. 2001. The origin of the ankyrin repeat
714 region in Notch intracellular domains is critical for regulation of HES promoter activity. Mech
715 Dev 104:3-20.
716 63. James AC, Szot JO, Iyer K, Major JA, Pursglove SE, Chapman G, Dunwoodie SL. 2014. Notch4
717 reveals a novel mechanism regulating Notch signal transduction. Biochim Biophys Acta
718 1843:1272-84.
719 64. Yamaguchi N, Oyama T, Ito E, Satoh H, Azuma S, Hayashi M, Shimizu K, Honma R, Yanagisawa
720 Y, Nishikawa A, Kawamura M, Imai J-i, Ohwada S, Tatsuta K, Inoue J-i, Semba K, Watanabe S.
721 2008. NOTCH3 Signaling Pathway Plays Crucial Roles in the Proliferation of ErbB2-Negative
722 Human Breast Cancer Cells. Cancer Research 68:1881-1888.
723 65. Liu Z, Brunskill E, Varnum-Finney B, Zhang C, Zhang A, Jay PY, Bernstein I, Morimoto M,
724 Kopan R. 2015. The intracellular domains of Notch1 and Notch2 are functionally equivalent
725 during development and carcinogenesis. Development 142:2452-2463.
726 66. Giachino C, Boulay JL, Ivanek R, Alvarado A, Tostado C, Lugert S, Tchorz J, Coban M, Mariani
727 L, Bettler B, Lathia J, Frank S, Pfister S, Kool M, Taylor V. 2015. A Tumor Suppressor Function
728 for Notch Signaling in Forebrain Tumor Subtypes. Cancer Cell 28:730-742.
729 67. Rossi D, Trifonov V, Fangazio M, Bruscaggin A, Rasi S, Spina V, Monti S, Vaisitti T, Arruga F,
730 Famà R, Ciardullo C, Greco M, Cresta S, Piranda D, Holmes A, Fabbri G, Messina M, Rinaldi A,

731 Wang J, Agostinelli C, Piccaluga PP, Lucioni M, Tabbò F, Serra R, Franceschetti S, Deambrogi
732 C, Daniele G, Gattei V, Marasca R, Facchetti F, Arcaini L, Inghirami G, Bertoni F, Pileri SA,
733 Deaglio S, Foà R, Dalla-Favera R, Pasqualucci L, Rabadan R, Gaidano G. 2012. The coding
734 genome of splenic marginal zone lymphoma: activation of NOTCH2 and other pathways
735 regulating marginal zone development. Journal of Experimental Medicine 209:1537-1551.
736 68. De Strooper B, Annaert W, Cupers P, Saftig P, Craessaerts K, Mumm JS, Schroeter EH, Schrijvers
737 V, Wolfe MS, Ray WJ, Goate A, Kopan R. 1999. A presenilin-1-dependent γ-secretase-like
738 protease mediates release of Notch intracellular domain. Nature 398:518-522.
739 69. Lin SE, Oyama T, Nagase T, Harigaya K, Kitagawa M. 2002. Identification of new human
740 mastermind proteins defines a family that consists of positive regulators for notch signaling. J Biol
741 Chem 277:50612-20.
742 70. Wu L, Sun T, Kobayashi K, Gao P, Griffin JD. 2002. Identification of a family of mastermind-like
743 transcriptional coactivators for mammalian notch receptors. Mol Cell Biol 22:7688-700.
744 71. DiMaio D. 2019. Small size, big impact: how studies of small DNA tumour viruses revolutionized
745 biology. Philos Trans R Soc Lond B Biol Sci 374:20180300.
746 72. Siebel C, Lendahl U. 2017. Notch Signaling in Development, Tissue Homeostasis, and Disease.
747 Physiol Rev 97:1235-1294.
748 73. Sprinzak D, Blacklow SC. 2021. Biophysics of Notch Signaling. Annu Rev Biophys 50:157-189.
749 74. Wang H, Zang C, Taing L, Arnett KL, Wong YJ, Pear WS, Blacklow SC, Liu XS, Aster JC. 2014.
750 NOTCH1-RBPJ complexes drive target gene expression through dynamic interactions with
751 superenhancers. Proc Natl Acad Sci U S A 111:705-10.
752 75. Castel D, Mourikis P, Bartels SJ, Brinkman AB, Tajbakhsh S, Stunnenberg HG. 2013. Dynamic
753 binding of RBPJ is determined by Notch signaling status. Genes Dev 27:1059-71.

754 76. Krejci A, Bray S. 2007. Notch activation stimulates transient and selective binding of Su(H)/CSL
755 to target enhancers. Genes Dev 21:1322-7.
756 77. Gomez-Lamarca MJ, Falo-Sanjuan J, Stojnic R, Abdul Rehman S, Muresan L, Jones ML, Pillidge
757 Z, Cerda-Moya G, Yuan Z, Baloul S, Valenti P, Bystricky K, Payre F, O'Holleran K, Kovall R,
758 Bray SJ. 2018. Activation of the Notch Signaling Pathway In Vivo Elicits Changes in CSL Nuclear
759 Dynamics. Developmental Cell 44:611-623.e7.
760 78. Zhao B, Zou J, Wang H, Johannsen E, Peng CW, Quackenbush J, Mar JC, Morton CC, Freedman
761 ML, Blacklow SC, Aster JC, Bernstein BE, Kieff E. 2011. Epstein-Barr virus exploits intrinsic B-
762 lymphocyte transcription programs to achieve immortal cell growth. Proc Natl Acad Sci U S A
763 108:14902-7.
764 79. Severson E, Arnett KL, Wang H, Zang C, Taing L, Liu H, Pear WS, Shirley Liu X, Blacklow SC,
765 Aster JC. 2017. Genome-wide identification and characterization of Notch transcription complex–
766 binding sequence-paired sites in leukemia cells. Science Signaling 10:eaag1598.
767 80. Ryan RJH, Petrovic J, Rausch DM, Zhou Y, Lareau CA, Kluk MJ, Christie AL, Lee WY, Tarjan
768 DR, Guo B, Donohue LKH, Gillespie SM, Nardi V, Hochberg EP, Blacklow SC, Weinstock DM,
769 Faryabi RB, Bernstein BE, Aster JC, Pear WS. 2017. A B Cell Regulome Links Notch to
770 Downstream Oncogenic Pathways in Small B Cell Lymphomas. Cell Reports 21:784-797.
771 81. Yashiro-Ohtani Y, Wang H, Zang C, Arnett KL, Bailis W, Ho Y, Knoechel B, Lanauze C, Louis
772 L, Forsyth KS, Chen S, Chung Y, Schug J, Blobel GA, Liebhaber SA, Bernstein BE, Blacklow
773 SC, Liu XS, Aster JC, Pear WS. 2014. Long-range enhancer activity determines Myc
774 sensitivity to Notch inhibitors in T cell leukemia. Proceedings of the National Academy of
775 Sciences doi:10.1073/pnas.1407079111:201407079.
776 82. Song M, Brown H, Wu T-T, Sun R. 2001. Transcription activation of polyadenylated nuclear RNA
777 by Rta in Human herpesvirus 8/Kaposi's Sarcoma-associated herpesvirus. J Virol 75:3129-40.

778 83. Chen J, Ye F, Xie J, Kuhne K, Gao SJ. 2009. Genome-wide identification of binding sites for
779 Kaposi's sarcoma-associated herpesvirus lytic switch protein, RTA. Virology 386:290-302.
780 84. Wang Y, Li H, Chan MY, Zhu FX, Lukac DM, Yuan Y. 2004. Kaposi's sarcoma-associated
781 herpesvirus ori-Lyt-dependent DNA replication: cis-acting requirements for replication and ori-
782 Lyt-associated RNA transcription. J Virol 78:8615-29.
783 85. Rossetto CC, Susilarini NK, Pari GS. 2011. Interaction of Kaposi's sarcoma-associated herpesvirus
784 ORF59 with oriLyt is dependent on binding with K-Rta. J Virol 85:3833-41.
785 86. Papp B, Motlagh N, Smindak RJ, Jin Jang S, Sharma A, Alonso JD, Toth Z. 2019. Genome-Wide
786 Identification of Direct RTA Targets Reveals Key Host Factors for Kaposi's Sarcoma-Associated
787 Herpesvirus Lytic Reactivation. J Virol 93.
788 87. Castro B, Barolo S, Bailey AM, Posakony JW. 2005. Lateral inhibition in proneural clusters: cis-
789 regulatory logic and default repression by Suppressor of Hairless. Development 132:3333-3344.
790 88. Nellesen DT, Lai EC, Posakony JW. 1999. Discrete enhancer elements mediate selective
791 responsiveness of enhancer of split complex genes to common transcriptional activators. Dev Biol
792 213:33-53.
793 89. Wang H, Zou J, Zhao B, Johannsen E, Ashworth T, Wong H, Pear WS, Schug J, Blacklow SC,
794 Arnett KL, Bernstein BE, Kieff E, Aster JC. 2011. Genome-wide analysis reveals conserved and
795 divergent features of Notch1/RBPJ binding in human and murine T-lymphoblastic leukemia cells.
796 Proc Natl Acad Sci U S A 108:14908-13.
797 90. Swanson CI, Evans NC, Barolo S. 2010. Structural rules and complex regulatory circuitry
798 constrain expression of a Notch- and EGFR-regulated eye enhancer. Dev Cell 18:359-70.
799 91. Cooper MT, Tyler DM, Furriols M, Chalkiadaki A, Delidakis C, Bray S. 2000. Spatially restricted
800 factors cooperate with notch in the regulation of Enhancer of split genes. Dev Biol 221:390-403.

801 92. Cave JW, Loh F, Surpris JW, Xia L, Caudy MA. 2005. A DNA transcription code for cell-specific
802 gene activation by notch signaling. Curr Biol 15:94-104.
803 93. Takebayashi K, Sasai Y, Sakai Y, Watanabe T, Nakanishi S, Kageyama R. 1994. Structure,
804 chromosomal locus, and promoter analysis of the gene encoding the mouse helix-loop-helix factor
805 HES-1. Negative autoregulation through the multiple N box elements. J Biol Chem 269:5150-6.
806 94. Basak O, Giachino C, Fiorini E, MacDonald HR, Taylor V. 2012. Neurogenic Subventricular Zone
807 Stem/Progenitor Cells Are Notch1-Dependent in Their Active But Not Quiescent State. The
808 Journal of Neuroscience 32:5654-5666.
809 95. Stoeck A, Lejnine S, Truong A, Pan L, Wang H, Zang C, Yuan J, Ware C, MacLean J, Garrett-
810 Engele PW, Kluk M, Laskey J, Haines BB, Moskaluk C, Zawel L, Fawell S, Gilliland G, Zhang
811 T, Kremer BE, Knoechel B, Bernstein BE, Pear WS, Liu XS, Aster JC, Sathyanarayanan S. 2014.
812 Discovery of biomarkers predictive of GSI response in triple-negative breast cancer and adenoid
813 cystic carcinoma. Cancer Discov 4:1154-67.
814 96. Krejcí A, Bernard F, Housden BE, Collins S, Bray SJ. 2009. Direct response to Notch activation:
815 signaling crosstalk and incoherent logic. Sci Signal 2:ra1.
816 97. Choi SH, Severson E, Pear WS, Liu XS, Aster JC, Blacklow SC. 2017. The common oncogenomic
817 program of NOTCH1 and NOTCH3 signaling in T-cell acute lymphoblastic leukemia. PLOS ONE
818 12:e0185762.
819 98. Bellavia D, Campese AF, Checquolo S, Balestri A, Biondi A, Cazzaniga G, Lendahl U, Fehling
820 HJ, Hayday AC, Frati L, von Boehmer H, Gulino A, Screpanti I. 2002. Combined expression of
821 pTα and Notch3 in T cell leukemia identifies the requirement of preTCR for leukemogenesis.
822 Proceedings of the National Academy of Sciences 99:3788-3793.

823 99. Engler A, Rolando C, Giachino C, Saotome I, Erni A, Brien C, Zhang R, Zimber-Strobl U, Radtke
824 F, Artavanis-Tsakonas S, Louvi A, Taylor V. 2018. Notch2 Signaling Maintains NSC Quiescence
825 in the Murine Ventricular-Subventricular Zone. Cell Reports 22:992-1002.
826 100. Meester JAN, Verstraeten A, Alaerts M, Schepers D, Van Laer L, Loeys BL. 2019. Overlapping
827 but distinct roles for NOTCH receptors in human cardiovascular disease. Clinical Genetics 95:85-
828 94.
829 101. Beatus P, Lundkvist J, Oberg C, Lendahl U. 1999. The notch 3 intracellular domain represses
830 notch 1-mediated activation through Hairy/Enhancer of split (HES) promoters. Development
831 126:3925-3935.
832 102. Beà S, Valdés-Mas R, Navarro A, Salaverria I, Martín-Garcia D, Jares P, Giné E, Pinyol M, Royo
833 C, Nadeu F, Conde L, Juan M, Clot G, Vizán P, Di Croce L, Puente DA, López-Guerra M, Moros
834 A, Roue G, Aymerich M, Villamor N, Colomo L, Martínez A, Valera A, Martín-Subero JI,
835 Amador V, Hernández L, Rozman M, Enjuanes A, Forcada P, Muntañola A, Hartmann EM,
836 Calasanz MJ, Rosenwald A, Ott G, Hernández-Rivas JM, Klapper W, Siebert R, Wiestner A,
837 Wilson WH, Colomer D, López-Guillermo A, López-Otín C, Puente XS, Campo E. 2013.
838 Landscape of somatic mutations and clonal evolution in mantle cell lymphoma. Proceedings of the
839 National Academy of Sciences 110:18250-18255.
840 103. Ables JL, DeCarolis NA, Johnson MA, Rivera PD, Gao Z, Cooper DC, Radtke F, Hsieh J, Eisch
841 AJ. 2010. Notch1 Is Required for Maintenance of the Reservoir of Adult Hippocampal Stem Cells.
842 The Journal of Neuroscience 30:10484-10492.
843 104. Nwabo Kamdje AH, Bassi G, Pacelli L, Malpeli G, Amati E, Nichele I, Pizzolo G, Krampera M.
844 2012. Role of stromal cell-mediated Notch signaling in CLL resistance to chemotherapy. Blood
845 Cancer Journal 2:e73-e73.

846 105. Demehri S, Turkoz A, Manivasagam S, Yockey Laura J, Turkoz M, Kopan R. 2012. Elevated
847 Epidermal Thymic Stromal Lymphopoietin Levels Establish an Antitumor Environment in the
848 Skin. Cancer Cell 22:494-505.
849 106. Boucher JM, Harrington A, Rostama B, Lindner V, Liaw L. 2013. A Receptor-Specific Function
850 for Notch2 in Mediating Vascular Smooth Muscle Cell Growth Arrest Through Cyclin-dependent
851 Kinase Inhibitor 1B. Circulation Research 113:975-985.
852 107. Southgate L, Sukalo M, Karountzos ASV, Taylor EJ, Collinson CS, Ruddy D, Snape KM,
853 Dallapiccola B, Tolmie JL, Joss S, Brancati F, Digilio MC, Graul-Neumann LM, Salviati L, Coerdt
854 W, Jacquemin E, Wuyts W, Zenker M, Machado RD, Trembath RC. 2015. Haploinsufficiency of
855 the NOTCH1 Receptor as a Cause of Adams–Oliver Syndrome With Variable Cardiac
856 Anomalies. Circulation: Cardiovascular Genetics 8:572-581.
857 108. Kawai H, Kawaguchi D, Kuebrich BD, Kitamoto T, Yamaguchi M, Gotoh Y, Furutachi S. 2017.
858 Area-Specific Regulation of Quiescent Neural Stem Cells by Notch3 in the Adult Mouse
859 Subependymal Zone. The Journal of Neuroscience 37:11867-11880.
860 109. Arasada RR, Amann JM, Rahman MA, Huppert SS, Carbone DP. 2014. EGFR blockade enriches
861 for lung cancer stem-like cells through Notch3-dependent signaling. Cancer Research
862 doi:10.1158/0008-5472.Can-13-3724:canres.3724.2013.
863 110. Kofler NM, Cuervo H, Uh MK, Murtomäki A, Kitajewski J. 2015. Combined deficiency of Notch1
864 and Notch3 causes pericyte dysfunction, models CADASIL and results in arteriovenous
865 malformations. Scientific Reports 5:16449.
866 111. Arruga F, Vaisitti T, Deaglio S. 2018. The NOTCH Pathway and Its Mutations in Mature B Cell
867 Malignancies. Frontiers in Oncology 8.
868 112. Parmigiani E, Taylor V, Giachino C. 2020. Oncogenic and Tumor-Suppressive Functions of
869 NOTCH Signaling in Glioma. Cells 9:2304.

870 113. D'Assoro AB, Leon-Ferre R, Braune EB, Lendahl U. 2022. Roles of Notch Signaling in the Tumor
871 Microenvironment. Int J Mol Sci 23.
872 114. Nam Y, Sliz P, Pear WS, Aster JC, Blacklow SC. 2007. Cooperative assembly of higher-order
873 Notch complexes functions as a switch to induce transcription. Proc Natl Acad Sci U S A
874 104:2103-8.
875 115. Nam Y, Sliz P, Song L, Aster JC, Blacklow SC. 2006. Structural basis for cooperativity in
876 recruitment of MAML coactivators to Notch transcription complexes. Cell 124:973-83.
877 116. Arnett KL, Hass M, McArthur DG, Ilagan MX, Aster JC, Kopan R, Blacklow SC. 2010. Structural
878 and mechanistic insights into cooperative assembly of dimeric Notch transcription complexes. Nat
879 Struct Mol Biol 17:1312-7.
880 117. Liu H, Chi AW, Arnett KL, Chiang MY, Xu L, Shestova O, Wang H, Li YM, Bhandoola A, Aster
881 JC, Blacklow SC, Pear WS. 2010. Notch dimerization is required for leukemogenesis and T-cell
882 development. Genes Dev 24:2395-407.

883

884

885 **FIGURE LEGENDS**

886 **Figure 1. Endogenous Notch1 is constitutively active in infected Vero cells.** Total cellular protein
887 was harvested in RIPA buffer from triplicate cultures of 4 x 10^5 cells Vero rKSHV.294 cells at time of
888 plating ("0h") or 24h after plating. 20 ugs from each extract were separated on a 4-12% PAGE gradient
889 gel electrophoresed in Tris-MOPS-SDS buffer. The NICD1 control lane ("Con") contains equal total
890 protein from uninfected Vero cells transfected with NICD1 expression vector pCMV-NICD1. Proteins
891 transferred to nitrocellulose were probed with Notch1-specific bTAN20 antibody (1:500) or anti-GAPDH
892 antibody (1:5000), followed by HRP-conjugated anti-Rat secondary antibody (1:5000). Bands were
893 visualized by ChemiDoc (BioRad).

894
895
896 **Figure 2. Notch inhibition reduces Rta-mediated reactivation without inhibiting cell growth.**
897
898 **A. Treatment with a gamma secretase inhibitor decreases viral reactivation by Rta.** Vero
899 rKSHV.294 cells were treated with 1 or 5 uM DAPT, or vehicle control ("Vh") 24h prior to transfection
900 with 2.5 ug of Rta expression vector. At 72h post-transfection, infectious virus was quantitated by
901 transferring the media to the 293 MSR tet-OFF complementing reporter cells as described in Methods.
902 SeAP was measured in 25 uL of media per infection using the Phospha-Light System (Applied
903 Biosystems). SeAP values from media alone were subtracted from each experimental value, and folds
904 were calculated by normalizing to samples treated with vehicle and transfected with empty vector.
905 *$p<0.05$ by t test compared to Vec + Vh.

906 B. **Treatment with a gamma secretase inhibitor decreases activity of a Notch-dependent**
907 **reporter plasmid.** Vero rKSHV.294 cells were transfected with Notch reporter plasmid pGL2-4xCSL
908 expressing firefly luciferase ("Jk") and pcDNA3.1-HisLacZ expressing β-galactosidase ("Cont"). Cells
909 were treated with 5 uM DAPT or vehicle (DMSO) 24hr post-transfection, and total cellular protein was
910 extracted. Luciferase values were normalized to βgal values at each timepoint. *$p<0.0015$ and
911 **$p<0.0001$ by t test compared to Cont at each time point.

912 C. **Notch inhibition by DAPT treatment does not affect Vero rKSHV.294 cell growth.**
913 Triplicate cultures of Vero rKSHV.294 cells were treated with vehicle or DAPT at the indicated
914 concentrations, in triplicate, as described in Fig 2A. At the post-treatment times indicated, cell viability
915 was quantitated using Alamar Blue (BioRad). Mock values were averaged and subtracted from each
916 experimental value to yield corrected values. All corrected values were then normalized to 0h values
917 that had been set to the relative value of 1 for each treatment. The slight enhancement of cell growth rate
918 when compared to the vehicle control was not statistically-significant

919

920 **Fig 3. Inhibition of endogenous Notch by dominant negative MAML1 mutants inhibit viral**
921 **reactivation and expression of some viral genes. A.** Vero rKSHV.294 cells were transfected with 1ug
922 of plasmids expressing Rta and two different dnMAML alleles ("dnMAM" "A" and "B"; each fused to
923 GFP). Infectious virus was quantitated as in Fig. 2A. *p<0.02 and **p<0.01 by t test compared to Rta
924 plus Vector. **B. dnMAML1 proteins are well-expressed in infected Vero rKSHV.294 cells.** Vero
925 rKSHV.294 cells were transfected as in Fig 3A, total protein was harvested in RIPA buffer 48h later,
926 Western blotted, and probed with GFP-specific antiserum to detect the dnMAML-GFP fusion proteins.
927 As a control for the Western blot, plasmid expressing H2b-GFP was also transfected into cells. **C.**
928 **Expression of KSHV proteins are reduced by inhibiting endogenous Notch1.** Expression of the
929 KSHV proteins Mta, KbZIP, and ORF59 in extracts from cells transfected as in Fig 3B were visualized
930 by Western blotting. Fold induction of each viral protein was determined by normalizing to expression
931 of the host protein Histone H3 ("H3") in each lane, then dividing by the value for Vec alone, which had
932 been set to "1." D. **D.** Quantitation. The relative reduction of viral protein expression by inhibiting
933 Notch1 was calculated by comparing each viral protein's induction by ectopic Rta + Vec with that
934 induced by Rta in the presence of ectopic dnMAML1 in panel B. Rta alone was set at 100. *p<0.09 and
935 **p<0.005 by t test compared to Rta + Vec**. E. Expression of KSHV transcripts are reduced by**
936 **inhibiting endogenous Notch1.** Transcripts for the indicated viral genes were quantitated by real-time
937 quantitative reverse-transcription/PCR. Relative reduction of viral transcription by inhibiting Notch1
938 was calculated by the delta-delta Ct method comparing Rta + Vec or Rta + ectopic dnMAML1 and
939 cellular beta-actin transcription as the internal control. *p<0.1 and **p<0.05 by t test compared to Rta +
940 Vec**.**

941
942 **Fig 4. Activated Notch1 is required for optimal reactivation of KSHV. A. Reactivation by ectopic**
943 **Rta.** Vero rKSHV.294 cells were transfected with 30 pM of either scrambled siRNA (Scr; control),

944 Notch 1 siRNA A (N1-A), or Notch 1 siRNA B (N1-B) in triplicate sets. 48h later, Rta expression
945 vector or Vec (as control) was transfected into each of the siRNA-transfected cells. 48h post-
946 transfection, virus containing media were transferred to 293 MSR tet-OFF cells. Infectious virus was
947 quantitated as in Fig. 2A. *p<0.02 by t test compared to Rta + Scr **. B. Reactivation by VPA**
948 **treatment.** Vero rKSHV.294 cells were transfected with 30pM of either scrambled siRNA (Scr; control)
949 or Notch 1 siRNA B (N1-B). 54h later, 1 mM VPA was added to the siRNA-transfected cells. 72h
950 post-transfection, virus containing media were transferred to 293 MSR tet-OFF cells. Infectious virus
951 was quantitated as in Fig. 2A. **C. siRNA specifically reduces NICD1 expression.** Vero rKSHV.294
952 cells were transfected with 30pM of the siRNAs described in the legend to Fig. 4A. 48h post
953 transfection, total cellular proteins were extracted in RIPA buffer, then analyzed via a 10% SDS-
954 PAGE/western blot as described in the legend to Fig. 1A.
955
956
957 **Fig. 5. Activated Notch1 is required for optimal reactivation of KSHV in infected PEL cells. A.**
958 **DAPT inhibits vDNA accumulation in PEL cells.** Triplicate cultures of KSHV-infected BC3 cells were
959 treated with vehicle alone ("Vh") or containing 16, 32, or 40 uM DAPT for 65h. Total DNA was purified
960 using the FlexiGene DNA kit (Qiagen). Intracellular viral DNA was measured by real-time quantitative
961 (q) PCR using SYBR Green PCR Master Mix (Thermo Scientific) and GAPDH was the internal control.
962 Fold-DNA was calculated using the ΔCt method and all values were normalized to that of VPA + vehicle
963 alone, which was set to 100%. *p<0.03, **p<0.009, and ***p<0.006 by t test compared to VPA+Veh.
964 **B. Gene-specific expression of KSHV genes is reduced by Notch inhibition in PEL cells.** Triplicate
965 cultures of KSHV-infected BCBL1 cells were treated with 1 mM VPA and vehicle ("Vh") or DAPT (16,
966 32, or 40 uM). 48 or 72h post-treatment, ORF59 and K8.1 were detected by indirect immunofluorescence,
967 respectively. The percentages of ORF59 or K8.1 positive cells were quantitated, and fold-percent positive

968 cells were calculated by normalizing to samples treated with vehicle alone. *p<0.007 and **p<0.005 by
969 t test compared to VPA+Veh.
970
971
972 **Fig. 6. Ectopic NICD 1-4 are not sufficient to induce KSHV reactivation. A.** Vero rKSHV.294 cells
973 were transfected with 2.5 ug plasmid DNA expressing each of the indicated proteins and incubated for
974 72h at which time virus containing media were transferred to 293 MSR tet-OFF cells. Infectious virus
975 was quantitated as in the legend to Fig. 2A, using the Great EscAPe SeAP kit (Takara). T test was used
976 to determine that only samples transfected with Rta induced significant viral reactivation (p<0.05
977 compared to Vec). **B. All four constitutively active Notch isoforms are expressed ectopically in**
978 **transfected Vero rKSHV.294 cells.** Cells were transfected as in the legend to Fig 6A, and total proteins
979 were harvested in RIPA buffer 48h later, Western blotted, and probed with FLAG-tag and tubulin-specific
980 antibodies. All Notch isoforms were observed at the appropriate apparent MWs (46).
981
982 **Figure 7. Ectopic Notch isoforms 1 and 2 are transactivation competent in Vero rKSHV.294 cells.**
983 Triplicate cultures of Vero rKSHV.294 cells were transfected with 0.25 ug of the Notch reporter plasmid
984 4xCBS expressing firefly luciferase, control plasmid pcDNA3.1-HisLacZ expressing β-galactosidase
985 (βgal) and 3 ug of each of the four Notch isoform vectors. Extracts were made 48 h post-transfection, and
986 raw luciferase values were corrected to β-galactosidase. Folds were calculated by normalization to
987 samples transfected with luciferase reporter and empty vector (Vec) alone. *p<0.02 and **p<0.0001 by t
988 test compared to Vec.
989
990
991 **Figure 8. Ectopic NICD1 alleles with varying intrinsic activities are not sufficient to induce KSHV**
992 **reactivation.** Vero rKSHV.294 cells were transfected with 2.5 ug plasmid DNA expressing each of the
993 indicated proteins and incubated for 72h at which time virus containing media were transferred to 293

994 MSR tet-OFF cells. Infectious virus was quantitated as in Fig. 2A, using the Great EscAPe SeAP kit

995 (Takara).

996

997 **Fig. 9. Ectopic NICD1 cooperates with VPA in KSHV reactivation.** Vero rKSHV.294 cells were

998 transfected with 1 ug plasmid DNA expressing NICD1 ("N1") or empty vector. 18 h post-transfection,

999 cells were treated with 1 mM VPA. 72 h post-treatment, virus containing media were transferred to 293

1000 MSR tet-OFF cells. Infectious virus was quantitated as in Fig 2A.

DeCotiis-Mauro, et al., Fig 1

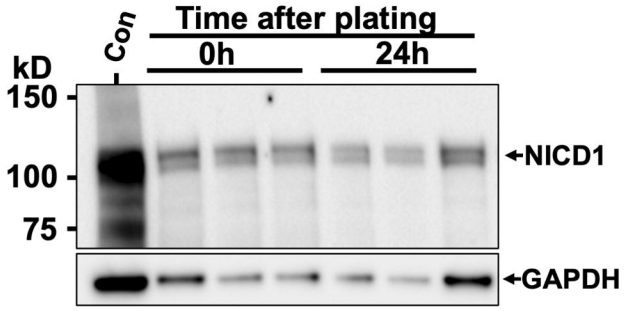

DeCotiis-Mauro, et al., Fig 2

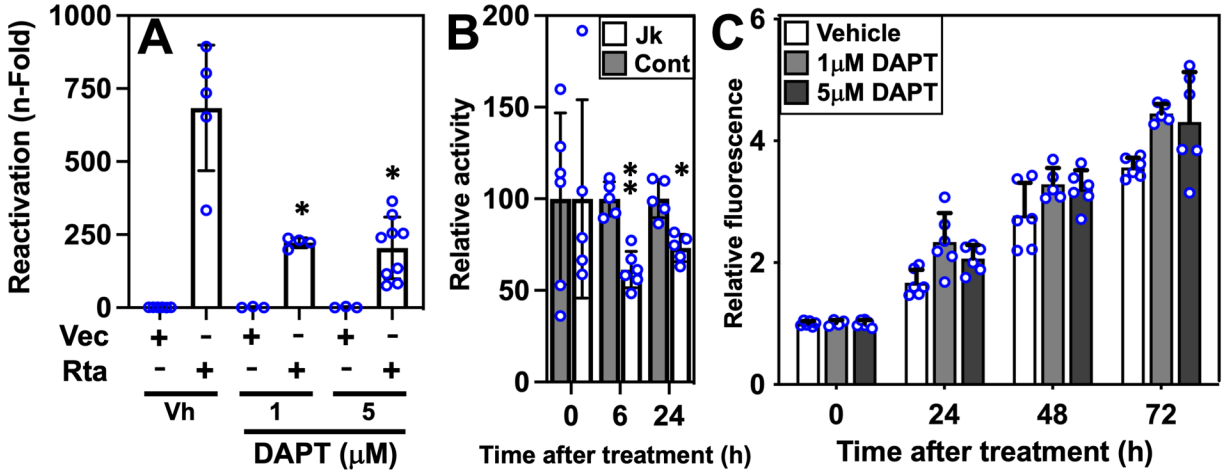

DeCotiis-Mauro, et al., Fig 3

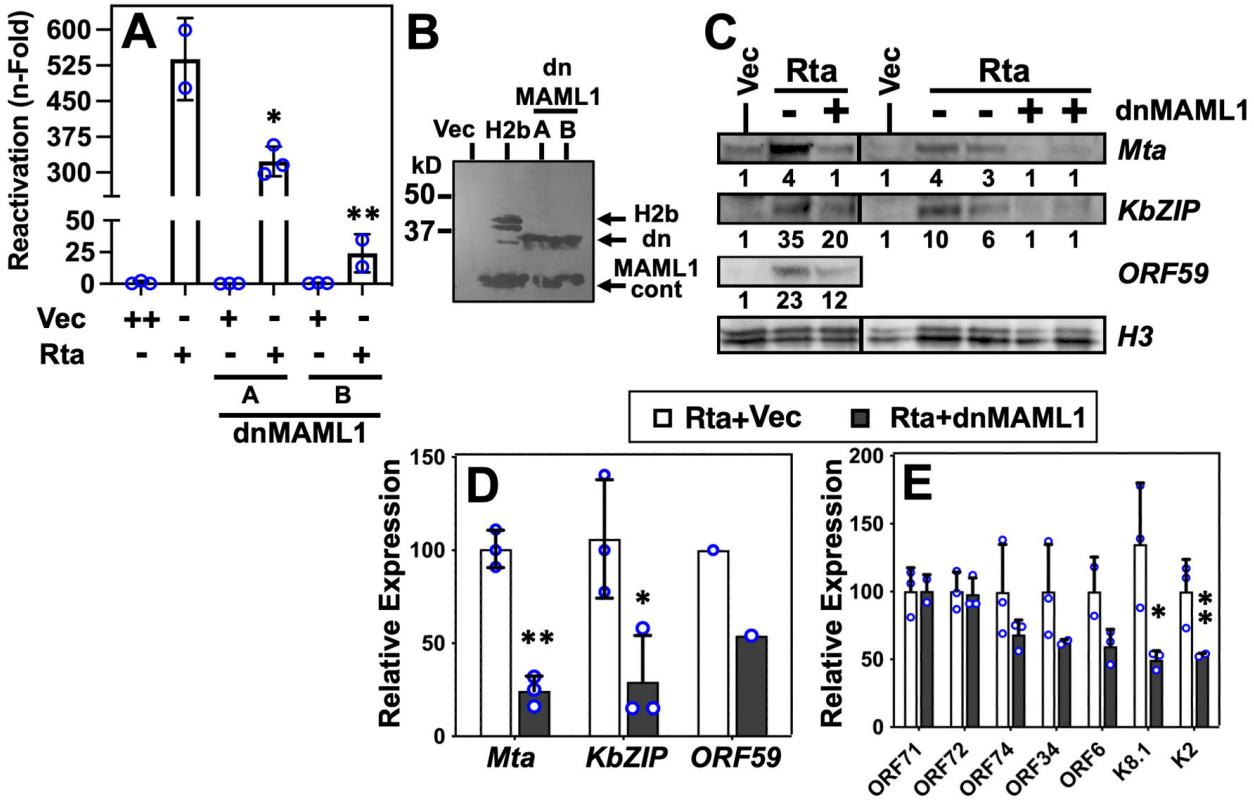

DeCotiis-Mauro, et al, Fig 4

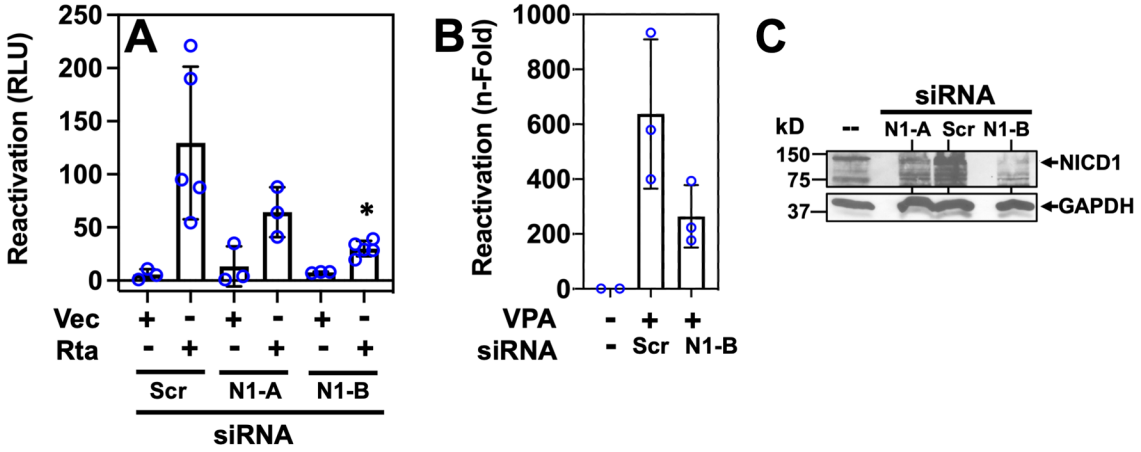

DeCotiis-Mauro, et al., Fig 5

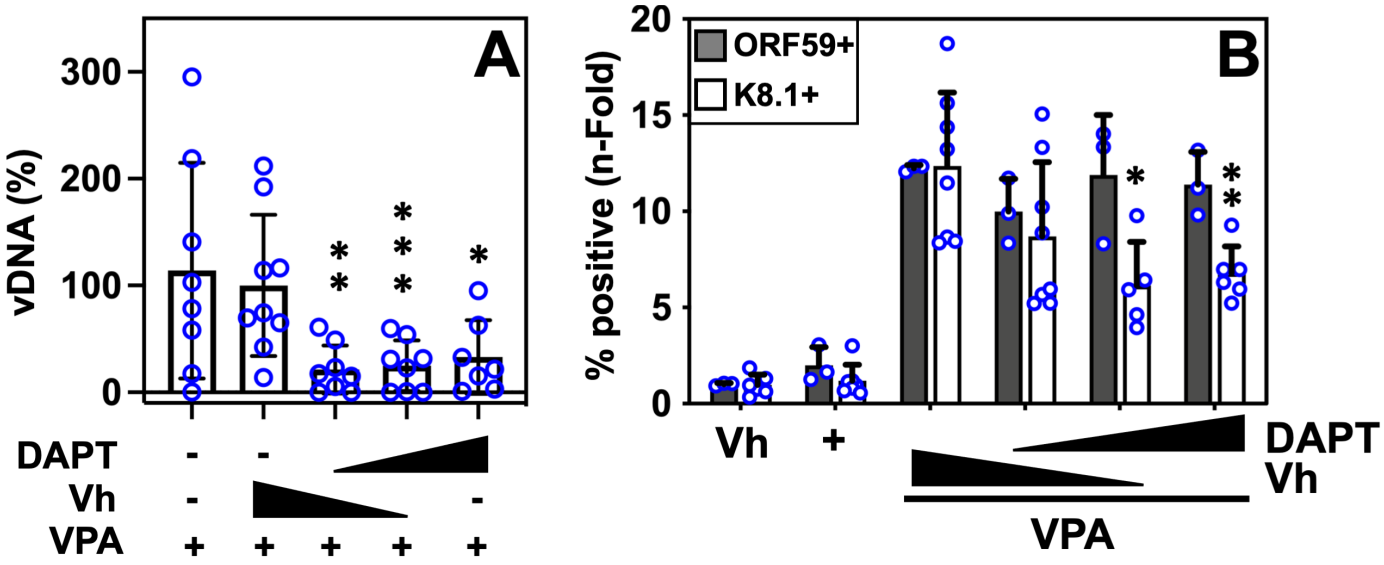

DeCotiis-Mauro, et al., Fig. 6

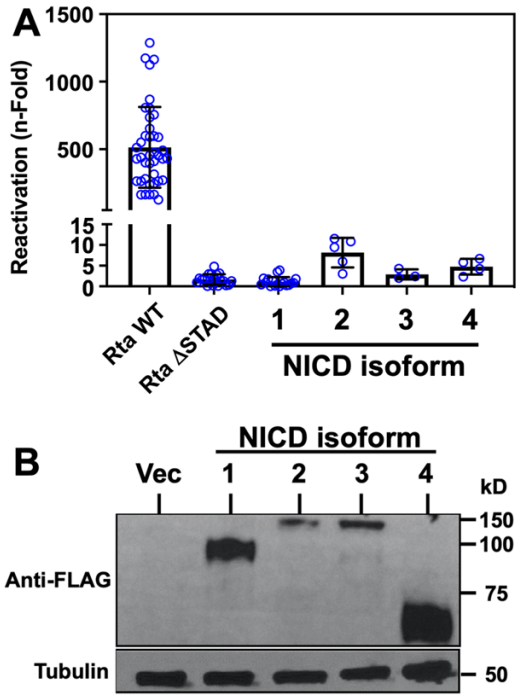

DeCotiis-Mauro, et al., Fig 7

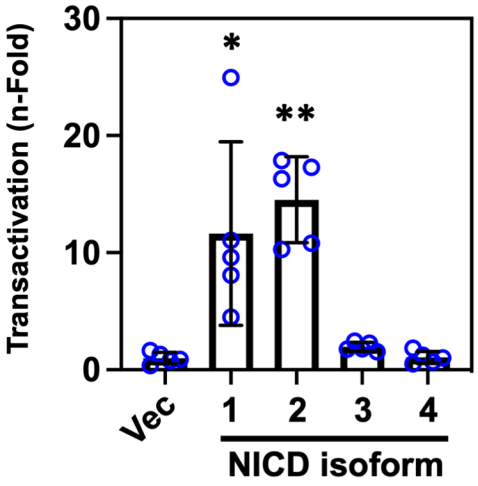

DeCotiis-Mauro, et al., Fig 8

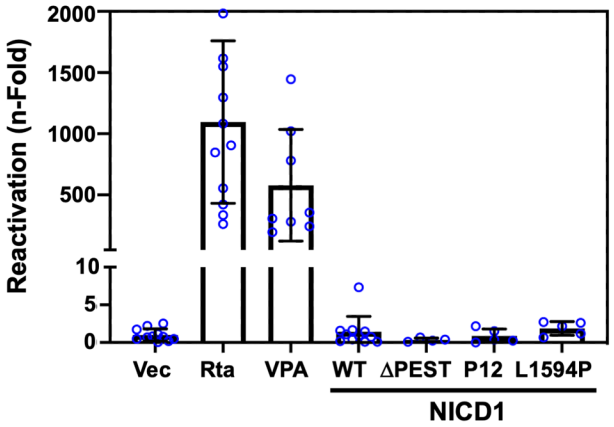
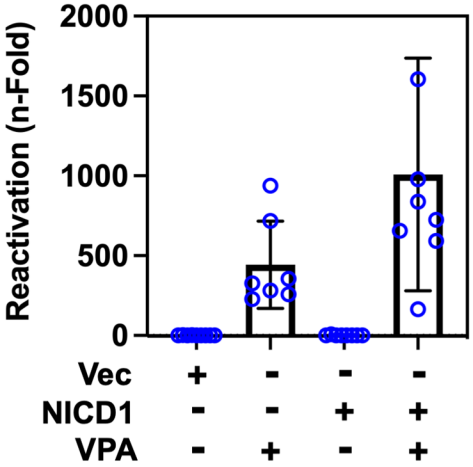
DeCotiis-Mauro, et al., Fig 9